



HAL
open science

Millennial-scale deglaciation across the European Alps at the transition between the Younger Dryas and the Early Holocene - evidence from a new cosmogenic nuclide chronology

Marie Protin, Irene Schimmelpfennig, Jean-louis Mugnier, Jean-françois Buoncristiani, Melaine Le Roy, Benjamin Pohl, Luc Moreau

► To cite this version:

Marie Protin, Irene Schimmelpfennig, Jean-louis Mugnier, Jean-françois Buoncristiani, Melaine Le Roy, et al.. Millennial-scale deglaciation across the European Alps at the transition between the Younger Dryas and the Early Holocene - evidence from a new cosmogenic nuclide chronology. *Boreas*, 2021, 50 (3), pp.671-685. 10.1111/bor.12519 . hal-03290256v1

HAL Id: hal-03290256

<https://hal.science/hal-03290256v1>

Submitted on 22 Nov 2021 (v1), last revised 13 Jan 2022 (v2)

HAL is a multi-disciplinary open access archive for the deposit and dissemination of scientific research documents, whether they are published or not. The documents may come from teaching and research institutions in France or abroad, or from public or private research centers.

L'archive ouverte pluridisciplinaire **HAL**, est destinée au dépôt et à la diffusion de documents scientifiques de niveau recherche, publiés ou non, émanant des établissements d'enseignement et de recherche français ou étrangers, des laboratoires publics ou privés.

1 **Millennial-scale deglaciation across the European Alps at the transition**
2 **between the Younger Dryas and the Early Holocene – evidence from a new**
3 **cosmogenic nuclide chronology**

4

5 Marie Protin, Irene Schimmelpfennig, Jean-Louis Mugnier, Jean-François Buoncristiani,
6 Melaine Le Roy, Benjamin Pohl, Luc Moreau and ASTER Team

7

8 The reconstruction of mountain glacier response to rapid climate change in the past allows
9 accessing the effects of current climate change. Yet, the spatial and temporal variability of past
10 glacier fluctuations is not fully understood. In this study, we address the timing of glacier
11 fluctuations in the European Alps during the Younger Dryas/Early Holocene (YD/EH)
12 transition. In an effort to elucidate whether glacier fluctuations were synchronous during this
13 period, we present a new chronology of the Alpine Talèfre glacier, based on 14 new *in situ*-
14 produced cosmogenic ^{10}Be ages of moraines and roches moutonnées. The retreat of Talèfre
15 glacier was initiated during the mid-YD (~12.4 ka), then it experienced a gradual retreat
16 punctuated by at least 3 oscillations until ~11 ka before shrinking substantially within its Little
17 Ice Age limits (13th-19th century). Comparison of our findings with published glacier
18 chronologies in the Alpine region highlights broadly synchronous behavior of glaciers across
19 the Alps between 12 and 10 ka. The coeval glacier fluctuations at a regional scale suggest that
20 common regional climate conditions had a major impact on Alpine glacier variations during
21 the YD/EH transition. The similarity of glacier behavior and independent temperature records
22 in both the Alpine region and the Northern high latitudes suggests a teleconnection between
23 these regions, but differences in the amplitude of the mean annual versus summer temperature
24 signals point to pronounced changes in seasonality between the YD and the EH.

25

26 **Keywords**

27 Younger Dryas/Early Holocene transition; European Alps; Cosmogenic nuclide dating; Glacier
28 fluctuations.

29

30 *Marie Protin [marie.protin@univ-lorraine.fr], Aix-Marseille Univ, CNRS, IRD, INRA, Coll*
31 *France, CEREGE, Aix en Provence, France and Université de Lorraine, CNRS, CRPG, F-*
32 *54000 Nancy, France ; Irene Schimmelpfennig [schimmelpfennig@cerege.fr] and ASTER*
33 *Team (Georges Aumaître [aumaitre@cerege.fr], Didier Bourlès, [bourles@cerege.fr], Karim*
34 *Keddadouche [keddadouche@cerege.fr]), Aix-Marseille Univ, CNRS, IRD, INRA, Coll France,*
35 *CEREGE, Aix en Provence, France; Jean-Louis Mugnier [jean-louis.mugnier@univ-smb.fr],*
36 *Université Grenoble Alpes, Université Savoie Mont Blanc, CNRS, ISTerre, 73000 Chambéry,*
37 *France ; Jean-François Buoncristiani [jfbuon@u-bourgogne.fr] and Benjamin Pohl*
38 *[benjamin.pohl@u-bourgogne.fr], Biogéosciences, UMR 6282 CNRS, Université Bourgogne*
39 *Franche-Comté, 6 Boulevard Gabriel, 21000 Dijon, France ; Melaine Le Roy*
40 *[melaine.leroy@unige.ch], University of Geneva, Institute for Environmental Sciences,*
41 *Climate Change Impacts and Risks in the Anthropocene (C-CIA), CH-1205 Geneva,*
42 *Switzerland and Université Grenoble Alpes, Université Savoie Mont Blanc, CNRS, EDYTEM,*
43 *73000 Chambéry, France ; Luc Moreau [moreauluc@chx.fr], Université Grenoble Alpes,*
44 *Université Savoie Mont Blanc, CNRS, EDYTEM, 73000 Chambéry, France.*

45 Mountain glaciers are recognized as sensitive recorders of climate variability, and their
 46 fluctuations mainly depend on variations of both temperature during the melt season and snowy
 47 precipitation (Oerlemans, 2005; Roe et al., 2017). ~~In the case of the alpine glaciers, their recent~~
 48 ~~evolution~~ shows that ~~it their recent evolution~~ is controlled by large scale climate variations
 49 moderated by local specific factors (Rabatel et al., 2013; Vincent et al., 2017). In the light of
 50 current climate evolution and rapid retreat of glaciers worldwide, it is important to improve our
 51 understanding of the sensitivity of glaciers to rapid climate changes in the past, such as those
 52 during the Younger Dryas/Early Holocene (YD/EH) transition (between ~12 to 10 ka).
 53 Therefore, the impact of large-scale climate variations versus local climate and site-specific
 54 factors has to be better assessed by constraining past glacial chronologies.

55 Moraines and roches moutonnées represent clear geomorphic markers of past glacier extents.
 56 Studying and dating them is a valuable approach for constraining former glacier behavior,
 57 establishing glacier chronologies and investigating the related climate changes. Due to the lack
 58 of direct dating methods, the traditional chronology of glacier advances (“stadials”) in the Alps
 59 during the period of Late-Glacial and Early Holocene (EH) deglaciation is mainly based on
 60 comparative studies of moraine stratigraphies and morphologies and equilibrium line altitude
 61 (ELA) determinations (e.g. Maisch, 1981). The temporal correlations of these stadials with
 62 paleoclimatic periods were broadly confirmed by the pioneering cosmogenic nuclide studies at
 63 a few Alpine sites (see reviews in Ivy-Ochs, 2015; Ivy-Ochs et al., 2006). For instance, the
 64 Egesen stadial moraines are assigned to the Younger Dryas (YD) (from 12.9 to 11.7 ka;
 65 Rasmussen et al., 2006), and are associated with an ELA depression of 250-350m relative to
 66 the Little Ice Age (LIA) (Ivy-Ochs, 2015). The Kartell stadial moraines are assigned to the
 67 Preboreal cold oscillation (11.4 – 11.3 ka; Kobashi et al., 2008) with an ELA depression of
 68 120m (Ivy-Ochs, 2015). However, recent studies showed that correlating moraines from
 69 different Alpine valleys solely based on the above-mentioned comparative criteria only is not

Commenté [MLR1]: Si tu parles des Alpes il faut mettre une majuscule à Alpine ici ... sinon ça désigne les glaciers de montagne en général

Commenté [MOU2]: Non, il faut pas rajouter ça, on a déjà « solely » dans la phrase

70 reliable, highlighting the need for direct moraine dating with cosmogenic nuclides when
71 comparing moraines from various sites (e.g. Boxleitner et al., 2019; Reitner et al., 2016).

72 Over the past few years, parameters for the calculations of cosmic ray exposure ages were
73 refined (e.g. Balco, 2017; Balco et al., 2009, 2008; Borchers et al., 2016; Martin et al., 2017;
74 Young et al., 2013) and an increasing number of cosmogenic nuclide dating studies from the
75 Alps have been published, providing evidence of multiple glacier fluctuations during the Late-
76 Glacial and the EH (e.g. Baroni et al., 2017; Moran et al., 2016b, 2016a; Schindelwig et al.,
77 2012). Attempts of identifying temporal or spatial trends in Alpine glacier behavior during the
78 Late-Glacial and EH have been made in earlier studies (Braumann et al., 2020; Chenet et al.,
79 2016; Schimmelpfennig et al., 2014). Although age uncertainties are generally too large to infer
80 clear trends, an abrupt glacier recession is not documented in the Alps at the very sharp
81 transition between YD and Holocene that is observed in Greenland ice cores with a $\sim 10^{\circ}\text{C}$
82 warming in less than one hundred years-.

83 Rather, previous studies suggested that EH glacier stillstands or advances in the Alps could be
84 a response to abrupt cold spells observed in Greenland ice cores (e.g. Ivy-Ochs et al., 2009;
85 Schimmelpfennig et al., 2014, 2012; Schindelwig et al., 2012), such as the Preboreal Oscillation
86 or a cold event notable at ~ 10.9 ka (Rasmussen et al., 2006; Vinther et al., 2006).

87 In the Western ~~part of the mountain range~~ Alps, ~~Alpine~~ glacier chronologies from this period
88 have for a long time been very scarce, but recent robust records and additional data from the
89 French Alps will now provide the opportunity to use the Alpine data set as a whole for a regional
90 analysis (Chenet et al., 2016; Cossart et al., 2012; Hofmann, 2018; Protin et al., 2019;
91 Schimmelpfennig et al., 2019; Le Roy et al., in prep). The chronological investigation of these
92 moraine chronologies might indeed allow for a better understanding of the large-scale
93 paleoclimatic conditions during a period for which proxy and model data still show diverging
94 temperature trends in both mid- and high latitudes: coupled ocean-atmosphere climate models

Commenté [MOU3]: Marie, l'ordre des citations suit normalement des règles strictes, à voir en fonction du journal – à vérifier de partout dans le texte (tu les as mis toujours dans l'ordre alphabétique, c'est sûr que c'est bon ?)

Commenté [MOU4]: C'est pas d'abord 2012,

Commenté [MLR5]: Je ne sais pas si tu peux citer ça ;;;

Commenté [MOU6R5]: Sinon, il faut citer notre poster Schimmelpfennig et al., 2019

95 (e.g. Buizert et al., 2014) failed to reproduce the abrupt warming at the end of [the](#) YD found in
96 North Atlantic and Greenland ice cores (e.g. Rasmussen et al., 2006; Shakun et al., 2015),
97 whereas continental temperature reconstructions based on biological proxies either fit with this
98 drastic warming (chironomid records in Heiri et al., 2015) or indicate a much more gradual
99 warming (e.g. pollen records in Marsicek et al., 2018; glacier chronologies in Rainsley et al.
100 2018, Young et al., 2020).

101 In this study, we provide a new glacier chronology in the French Alps by analyzing the Talèfre
102 glacier patterns during the deglaciation of the “Jardin de Talèfre”, one of the highest moraine
103 sites in the Alps (close to 3000 m) where a set of moraines is deposited above roches moutonnées.
104 We present new *in-situ* cosmogenic beryllium-10 (^{10}Be) ages of moraines and roches
105 moutonnées for this zone ([Fig. 1](#)) and compare these new data with published ^{10}Be glacial
106 chronologies from elsewhere in the European Alps, selected for their quality (e.g. number of
107 samples, dispersion of the ages) and re-calculated using uniform methods. Building on this
108 regional compilation, we evaluate (i) the possibility of a regional synchronicity of glacier
109 fluctuations during the multi-millennia period of the end of the YD and the beginning of the
110 Holocene (hereafter YD/EH transition), (ii) the impact of large-scale climate variations on
111 glacier patterns versus site-specific factors, (iii) the underlying climatic drivers in a regional
112 scale and their potential link with the high-latitudes, and (iv) the climatic significance of the
113 small fluctuation range of glacier extent between the YD and EH in the light of the significant
114 and abrupt climate change recorded in independent proxy records.

115

116 Study site

117 Talèfre glacier (45°54'N, 6°59'E) is a cirque glacier located in the French part of the Mont-
118 Blanc massif and ~~was~~ a major tributary of Mer de Glace glacier, the largest glacier in the
119 Mont-Blanc massif ([Fig. 1](#)). To the north is located the Argentière glacier, the second largest

120 glacier in the Mont-Blanc massif (Fig. 1~~Fig. 1~~). In 2008, Talèfre glacier covered an area of $\sim 8 \text{ km}^2$
 121 with a maximum length of 4.5 km and altitude spanning 2473 m to 3743 m a.s.l. (Gardent,
 122 2014). The ELA of Talèfre glacier for the period 1984-2010 was estimated to $\sim 3000 \text{ m}$ (Rabatel
 123 et al., 2013). Next to Argentière glacier, the mean annual temperature and precipitation for the
 124 time period 1979-2002 are estimated at 1.8°C and 1783 mm at $\sim 2000 \text{ m a.s.l.}$ (Joly et al., 2018
 125 and personal communication of D. Joly). The catchment of Talèfre glacier is ~~constrained~~
 126 bordered by hillsides-rock faces composed of granite rocks of late Hercynian age ($\sim 300 \text{ Ma}$;
 127 Bussy et al., 2000).

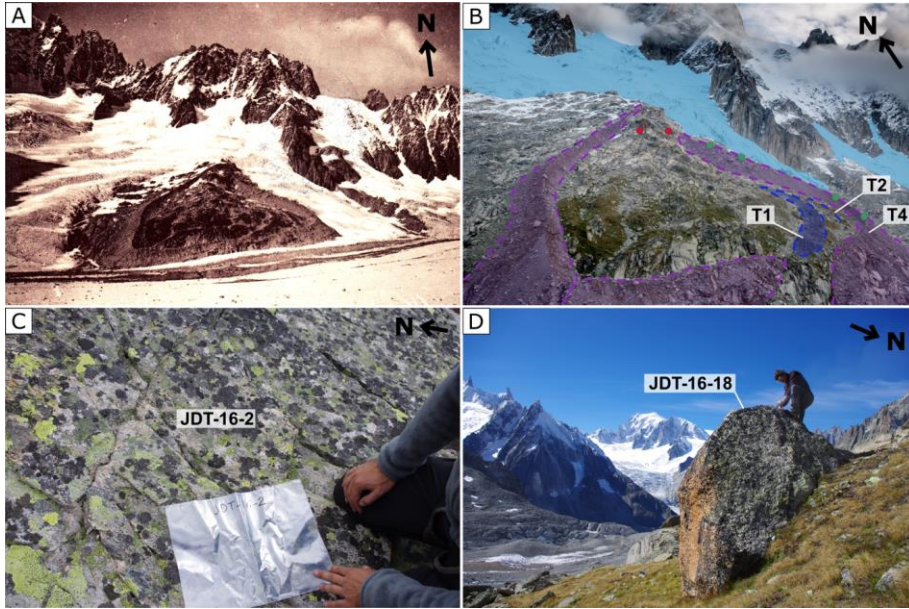
128 During the YD, Talefre glacier was connected to Mer de glace, which at that time occupied the
 129 Arve Valley with a front located westward of the left boundary of Fig. 1~~Fig. 1~~ (Prud'homme et al.,
 130 2020). During the last LIA advance in the 19th century, Talèfre glacier was confluent with
 131 Leschaux glacier, which then joins Tacul glacier to form Mer de Glace (Fig. 1~~Fig. 1~~). Since ~ 1950
 132 the Talèfre and Leschaux glaciers have not been coalescing (Gardent, 2014).

133 A notable feature of Talèfre glacier is the presence of a triangle-shaped rock islet at its center,
 134 named "Jardin de Talèfre" (i.e. Talèfre garden). This islet is bounded by moraines (

Commenté [MLR7]: La référence à citer pour le front de la MdG pendant le PAG est plutôt Nussbaumer et al 2007

Commenté [MOU8R7]: ? Mais ici on parle du YD... donc je pense que tu peux laisser comme ça

Commenté [MOU9]: Better « further downvalley »?



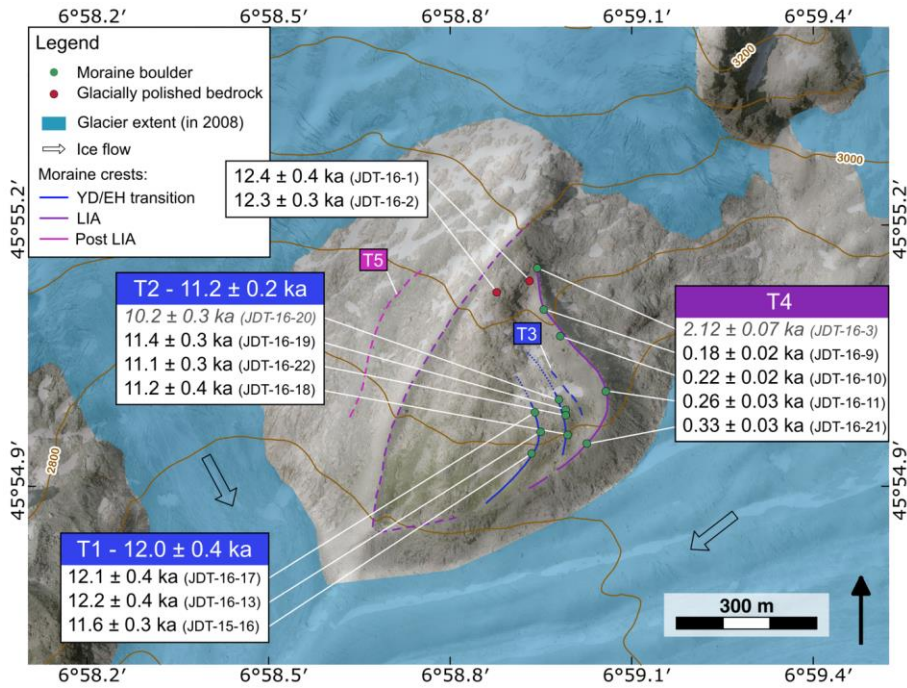
135
 136 [Fig. 2](#) (Fig. 2), that span 2640 m to 3040 m a.s.l. (Jordan, 2010). Because of its remoteness, this area
 137 has not been disturbed by human activity. According to the French État-Major maps (surveyed
 138 in 1820-1866) and first available photographs made by August-Rosalie Bisson in 1862 the
 139 “Jardin de Talèfre” was not ice-covered during the last LIA maximum (de Decker Hefltler,
 140 2002).

141

142 Methodology

143 *Moraine mapping*

144 Several so-far undated moraine ridges preserved on the islet were studied and represented in
 145 the geomorphologic map of

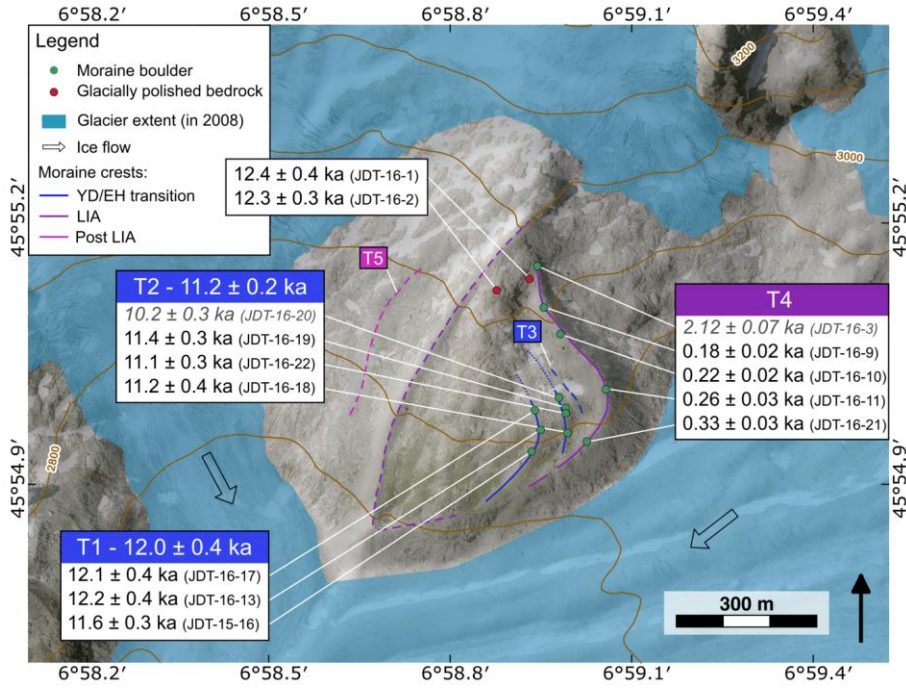


146
 147 Fig. 3 Fig-3. The mapping was realized through field work and interpretation of aerial images from
 148 the year 2015 (French national institute of geographic and forest information - IGN, 50 cm
 149 resolution).

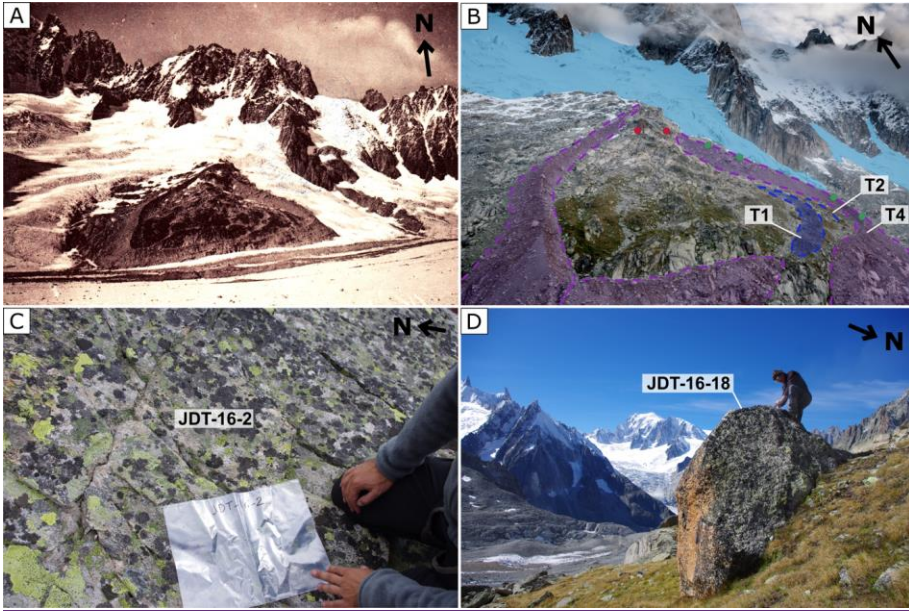
150

151 *Sample collection*

152 Fourteen samples were collected in the “Jardin de Talèfre”, two from smoothed bedrock
 153 surfaces resulting from glacial erosion and 12 from moraine boulders (

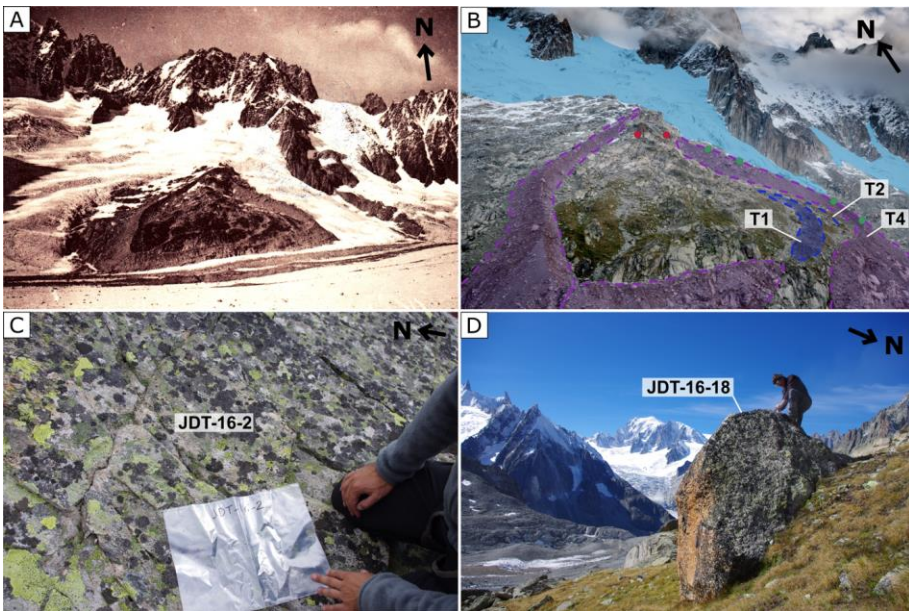


154
 155 Fig. 3 (Fig. 3). Bedrock samples were taken from the surface of the rocky islet, and attention was paid
 156 to avoid the possibility of cover by snow or vegetation and significant erosion by choosing
 157 sloping spots with glacial morphologies (



158

159 Fig. 2Fig. 2c). Both surfaces were covered by lichen. Moraine boulder samples were taken from the
160 top of the boulders, which were embedded in the crest or slope of the targeted moraines (



161

162 [Fig. 2](#)Fig-2d). If we assume uninterrupted surface exposure, the bedrock exposure ages indicate when
163 the “Jardin de Talèfre” became ice-free for the last time, while the boulder exposure ages
164 represent the timing of the glacier culmination and moraine stabilization (for detailed discussion
165 see section “Oscillation of Talèfre glacier since the Younger Dryas”). Samples were collected
166 using a chisel, a hammer and a cordless angle grinder, and topographic shielding was evaluated
167 in the field using a clinometer.

169 *Laboratory procedures*

170 All samples were processed at CEREGE (Aix-en-Provence, France). Samples were crushed and
171 sieved to collect the 250-500 μm fraction. Quartz was first concentrated by magnetic separation
172 and then isolated by successive leaching in a $\text{H}_2\text{SiF}_6/\text{HCl}$ mixture or by froth flotation when the
173 mineralogy allowed it. The obtained quartz fraction was leached at least two times in a 5% HF
174 - 5% HNO_3 solution, followed by 24h in ultra-sonic bath in a 1% HF - 1% HNO_3 solution in
175 order to remove any remaining feldspars and to clean the grains from atmospheric ^{10}Be . Purified
176 quartz was completely dissolved in concentrated HF after addition of ~ 0.1 g of an in-house ^9Be
177 carrier solution (3025 ± 9 ppm; Merchel et al., 2008). Beryllium was extracted by successive
178 alkaline precipitations of $\text{Be}(\text{OH})_2$ alternated with separation on anion and cation columns.
179 Samples were then oxidized at 700°C for one hour and the final BeO mixed with Nb powder
180 and loaded into nickel cathodes. Measurements of the $^{10}\text{Be}/^9\text{Be}$ ratios by accelerator mass
181 spectrometry (AMS) were conducted at the French national AMS facility ASTER (Arnold et
182 al., 2010). Samples were calibrated against in-house standard STD-11 [with a \$^{10}\text{Be}/^9\text{Be}\$ ratio](#)
183 [of \$\(1.191 \pm 0.013\) \times 10^{-11}\$](#) ; (Braucher et al., 2015) and a ^{10}Be half-life of [\(\$1.387 \pm 0.0012\$ \) \$\times 10^6\$](#)
184 years (Chmeleff et al., 2010; Korschinek et al., 2010). Analytical uncertainties combine ASTER
185 counting statistics and stability ($\sim 5\%$; Arnold et al., 2010) and machine blank correction. The

186 number of atoms ^{10}Be in the samples calculated from the corresponding $^{10}\text{Be}/^9\text{Be}$ ratios was
 187 then corrected from that of the chemical blanks, which had $^{10}\text{Be}/^9\text{Be}$ ratios of $3.38 \pm 0.49 \times 10^{-15}$
 188 and $3.48 \pm 0.50 \times 10^{-15}$ (Table 1).
 189

190 *Age calculations*

191 Surface exposure ages of the here presented new data were computed with the CREp online
 192 calculator (Martin et al., 2017) using the Lal-Stone time corrected scaling scheme Lm, the
 193 ERA40 atmospheric reanalyses and the Atmospheric ^{10}Be -based VDM for geomagnetic
 194 database (see Martin et al., 2017 and references therein). We applied the production rate of 4.10
 195 ± 0.10 atoms $^{10}\text{Be}\cdot\text{g}^{-1}\cdot\text{a}^{-1}$ established by Claude et al. (2014) as it is the only regional ^{10}Be
 196 production rate available for Alpine sites and it is identical to the global ^{10}Be production rate
 197 resulting from the ICE-D database linked to CREp (4.11 ± 0.19 atoms $^{10}\text{Be}\cdot\text{g}^{-1}\cdot\text{a}^{-1}$). The two
 198 other production rates often used for studies in the Alps, i.e. the northeast North America
 199 “NENA” production rate (Balco et al., 2009) and the “Arctic” production rate (Young et al.,
 200 2013), which is almost identical with the recent Scotland production rate (Putnam et al., 2019),
 201 would lead to ages older by less than 2% and 1%, respectively. For easy comparison, we present
 202 in Table 1 the ages calculated with both the regional regional production rate and the “Arctic”
 203 production rate. We did not apply a correction for snow shielding, as we do not have sufficient
 204 quantitative data on snowfall during the Holocene, and all sampled surfaces are in wind-
 205 exposed locations. We did not correct for potential erosion, as we were careful to sample
 206 surfaces with least possible erosion. Applying a correction for considerable snow cover
 207 assuming 50 cm of snow for six months (Chenet et al., 2016) would lead to ages older by 6%
 208 to 8%. Applying a correction for erosion corresponding to an erosion rate of $1 \text{ mm}\cdot\text{kr}^{-1}$ (André,
 209 2002) would result in ages older by less than 1%.

Commenté [MOU10]: Needs to be added in the table

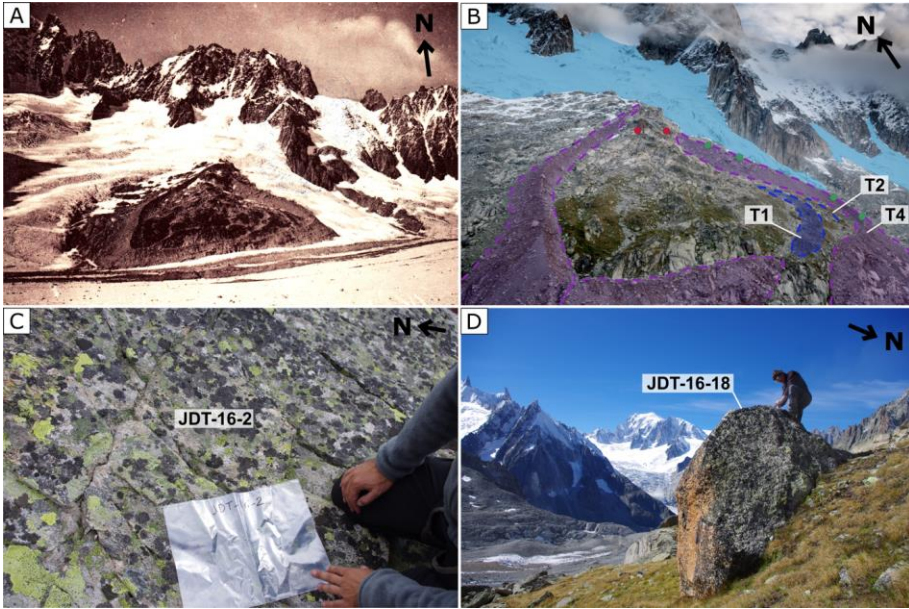
210 For the regional comparison of glacier records, previously published data from 18 study sites
211 (see references in Fig. 6) were homogenized by re-calculating the individual and mean ages
212 using the same procedures as above (Table S1). Boulders identified as outliers in the original
213 studies were kept as outliers. Applying the χ^2 test (2σ) by Ward and Wilson (1978) ~~above-~~
214 ~~mentioned χ^2 test~~, moraine age populations were tested for outliers, which were also discarded
215 as indicated in Table S1. Exceptions were made for the moraine M7a from the Rougnoux valley,
216 M2 from Falgin cirque and the lower moraine from Steingletscher, where all boulders (not
217 identified as outliers by authors) were kept for the mean age calculation even if they statistically
218 mismatch, as we do not have any argument for discarding a specific sample from the age
219 population. At the Rougnoux valley site, several moraine mean ages do not agree with the
220 stratigraphic order (M8-9, M7b, M4-5 and M6b) but these ages do not statistically differ;
221 therefore, we choose to include them all in the comparison. We eliminated from the comparison
222 the moraine ages that are based on only one sample and that have standard deviations >10% to
223 make the comparison as accurate as possible. Once this selection made, only the sites with at
224 least one moraine of Holocene age (< 11.7 ka) were kept for the comparison in order to exclude
225 sites with moraines that exclusively correspond to earlier Late-Glacial advances. Boxleitner et
226 al. (2019) dated 34 moraine boulders of several glacier systems in Meiental (central Alps), but
227 we deliberately did not consider the study in our test, because each moraine was dated with
228 only one boulder. Applying a realistic snow cover correction to all sites would equally shift all
229 moraine ages to slightly older dates and would not change the discussion.

230

231 Results

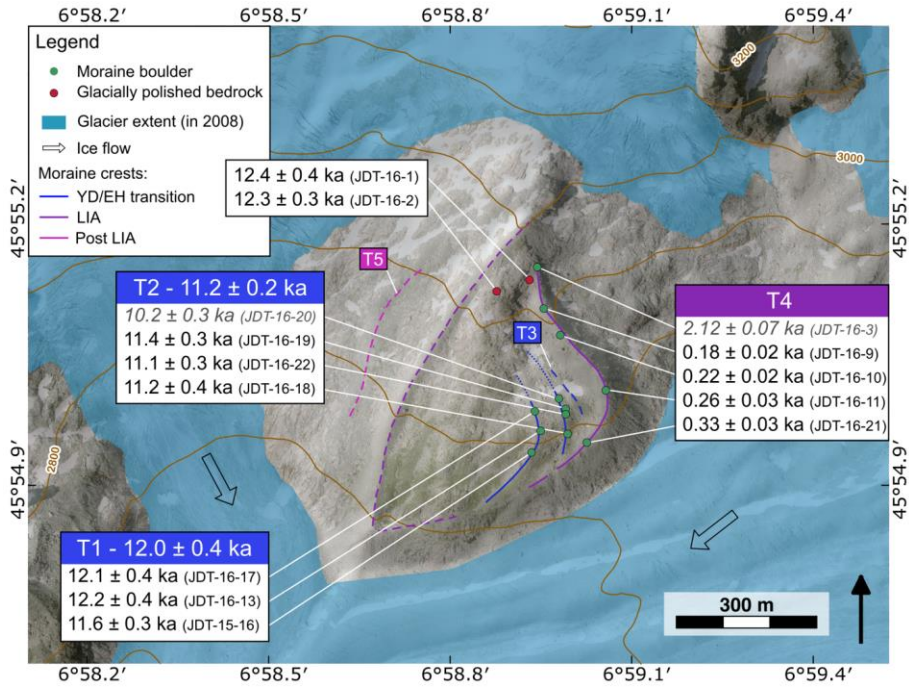
232 *Geomorphologic description of the [Talèfre](#) site*

233 Two massive lateral moraines, up to 50m high and 1km long, frame the islet [of the “Jardin de](#)
234 [Talèfre”](#) (purple moraines, including T4, in



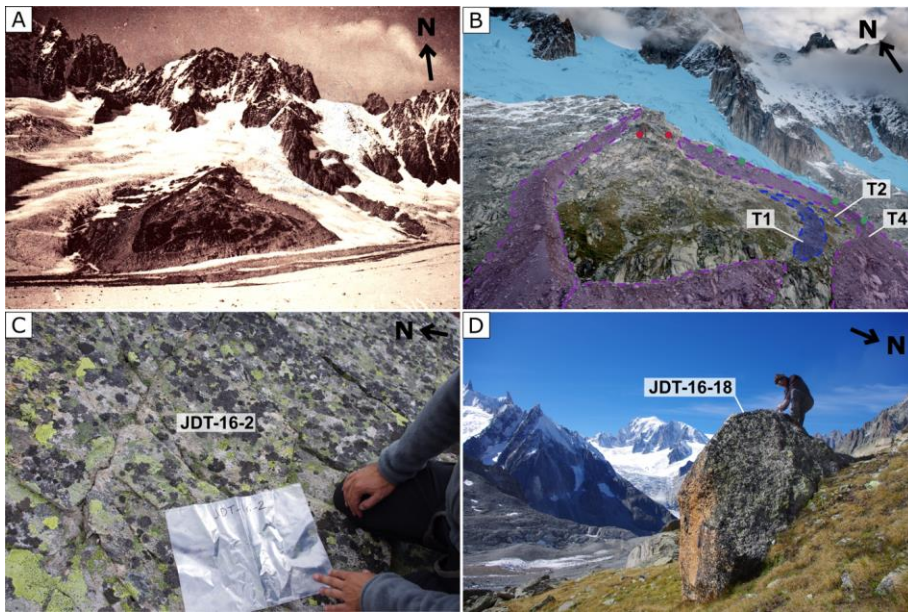
235

236 Fig. 2b and

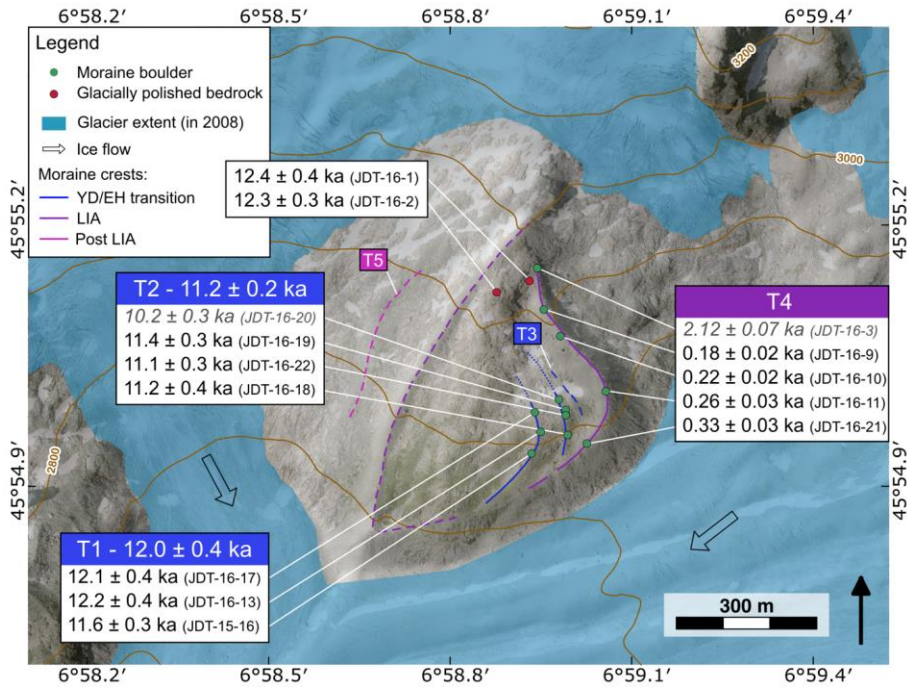


237

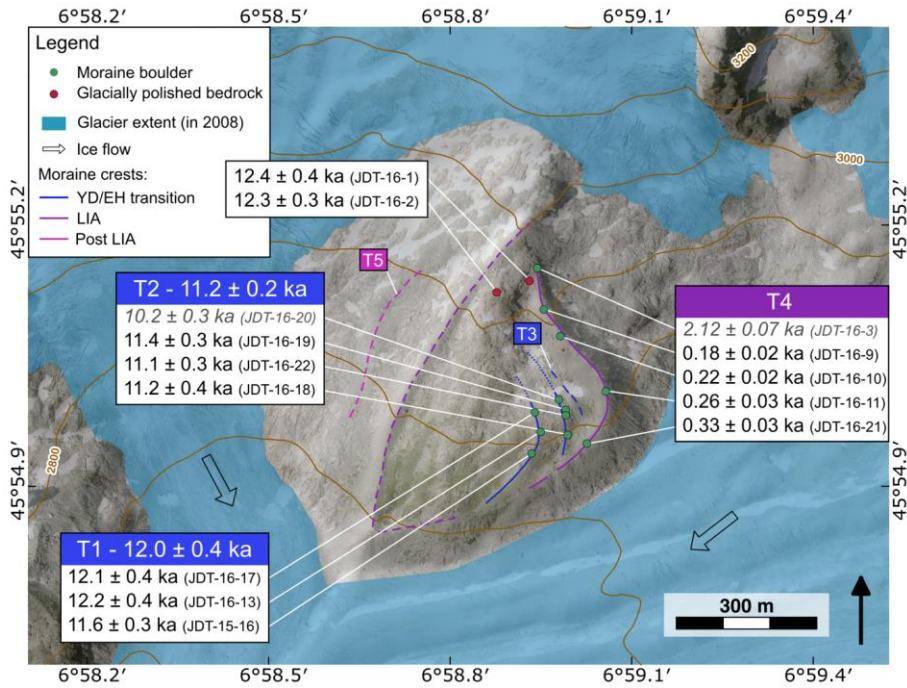
238 [Fig. 3](#) (Fig. 3). In the eastern part of the islet, three very smooth lateral moraine ridges (T1, T2 and T3)
 239 are visible in stratigraphically older location relative to the massive moraine T4 on the eastern
 240 margin. They are less than 2m high and between 100 and 200m long. The two outermost of
 241 these three moraine ridges (T1 and T2) bear several large boulders suitable for ^{10}Be dating,
 242 while the ridge T3 does not. These three ridges (T1 to T3) are represented in dark blue in



243
 244 [Fig. 2](#) (Fig. 2b) and



245
 246 **Fig. 3** Moraine mapping shows that they are leaning northward against a 20 m high rock slope
 247 at an altitude of ~2850m a.s.l.; to the south, they are crosscutted by the T4 moraine. Between
 248 the western massive ridge and the present glacier margin, a small ridge (T5) is visible (pink
 249 moraine in

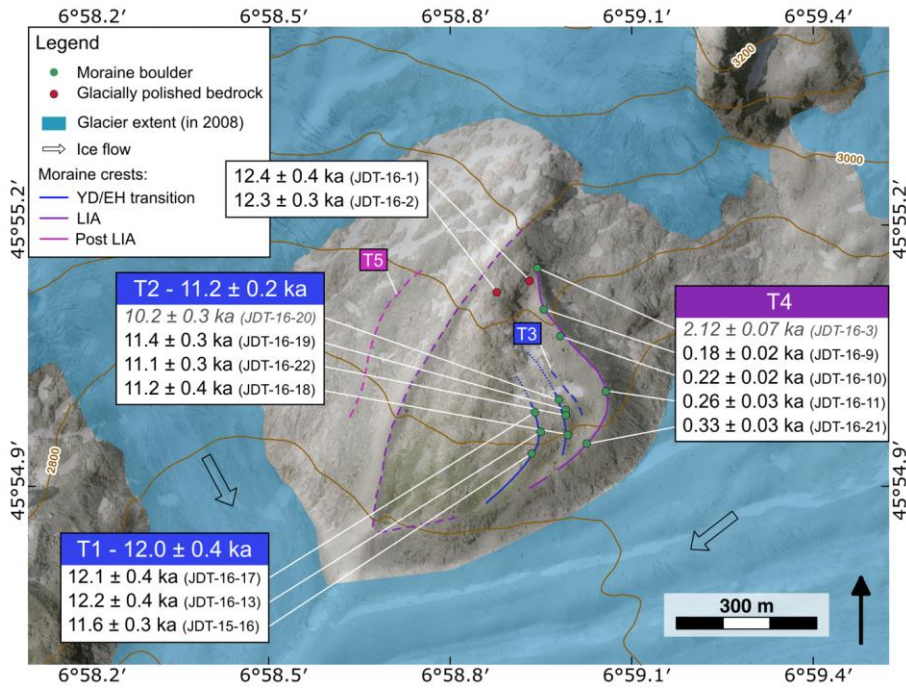


250
 251 [Fig. 3](#) Fig. 3). It has no equivalent on the eastern side and has been probably deposited during one of
 252 the short advances/stillstands that occurred at Alpine sites during the general glacier retreat of
 253 the 20th century (Braumann et al., 2020; Schimmelpfennig et al., 2014).

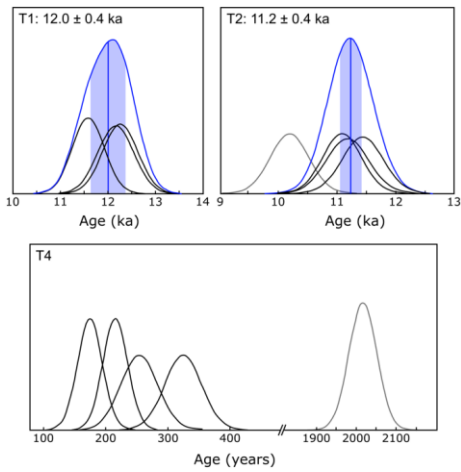
254

255 *Moraine and bedrock exposure ages of Talèfre glacier*

256 The two bedrock surfaces were sampled at the center of the northern part of “Jardin de Talèfre”.
 257 Moraine boulder samples were taken from three ridges in the eastern part of the islet, i.e. from
 258 the two stratigraphically outermost (oldest), smooth moraines T1 and T2, and from the
 259 innermost (youngest), massive moraine T4. Surface exposure ages are shown in



260
 261 [Fig. 3](#) and detailed in [Table 1](#). Probability plots of moraine boulder ages and arithmetic mean
 262 ages are shown in

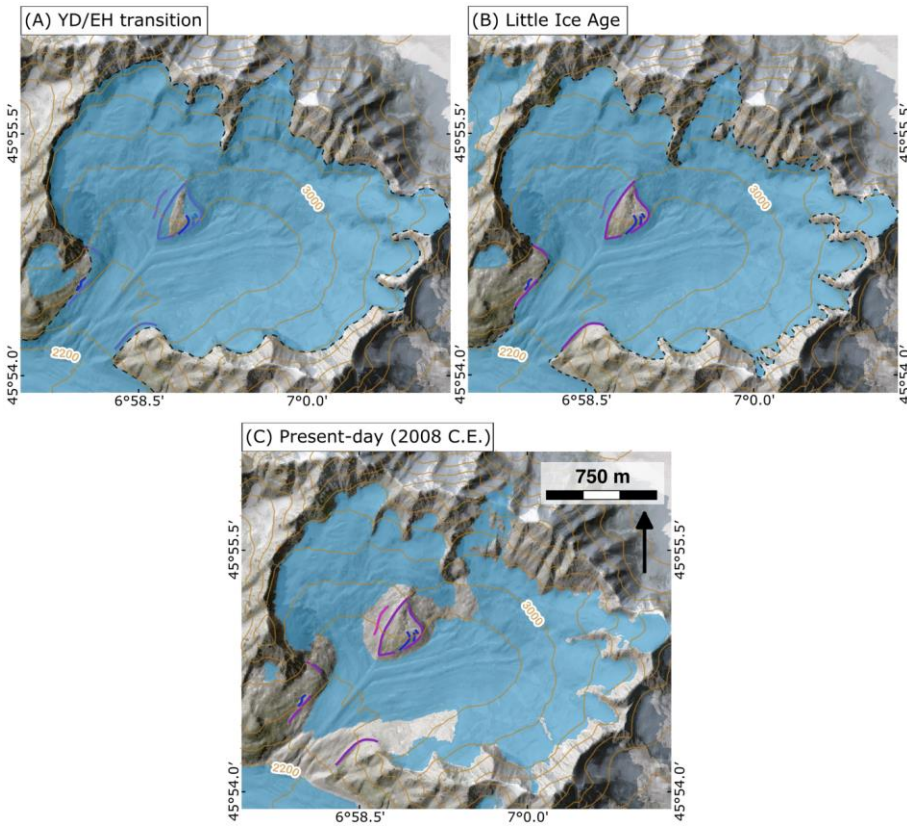


263
 18

264 [Fig. 4](#) Fig. 4. The consistency of individual ages within one moraine age populations were tested for
265 outliers with the χ^2 test (2σ) by Ward and Wilson (1978), using the analytical uncertainties of
266 the ages. In the text and in figures, individual ages are given with the analytical uncertainties,
267 to allow for internal comparison, and arithmetic mean ages are given with their standard
268 deviations, while Table 1 shows both analytical uncertainties and total uncertainties (including
269 the ^{10}Be rate uncertainty). See figure and table captions for details.

270 All ages are in agreement with their stratigraphic order. The two bedrock samples, JDT-16-1
271 and JDT-16-2, give indistinguishable exposure ages of 12.4 ± 0.4 ka and 12.3 ± 0.3 ka,
272 respectively. The three boulder ages from the outermost moraine T1 range between 12.2 ± 0.4
273 ka and 11.6 ± 0.3 ka, with a mean age of 12.0 ± 0.4 ka. Three boulder ages from moraine T2
274 are very well clustered between 11.4 ± 0.3 ka and 11.1 ± 0.3 ka and give a mean age of $11.2 \pm$
275 0.2 ka after discarding JDT-16-20 as an outlier (10.2 ± 0.3 ka). This boulder is less than 1m
276 high. It might thus have been exhumed or covered for a while by a layer of sediment, leading
277 to an underestimation of its exposure age. On the innermost moraine, four boulders yield ages
278 of 0.18 ± 0.02 ka, 0.22 ± 0.03 ka, 0.26 ± 0.02 ka and 0.33 ± 0.03 ka and one boulder is dated at
279 2.12 ± 0.07 ka.

280 According to this new set of exposure ages we propose a reconstruction of the past extents of
281 Talèfre glacier, corresponding to moraines T1 and T4 (



282
 283 [Fig. 5](#) Fig. 5). The mapping of the exterior glacier margins relies solely on remnants of undated
 284 moraines, assumed variations in relation to catchment slopes and 19th century maps from French
 285 État-Major.

286

287 *Exposure ages of the other Alpine chronologies*

288 The previously published 18 Alpine glacier chronologies that are considered here, are
 289 characterized by sets of lateral and/or latero-frontal moraines originally dated between ~13.5
 290 ka and ~9.5 ka. Of these 18 sites, eleven meet the quality criteria presented in the Methodology
 291 (see section “Age calculations”) and yield recalculated ¹⁰Be exposure ages between 14.5 ka and
 292 9.8 ka ~~ka~~. The moraine ages of the other sites are either older (Val Viola, Gesso della Barra

293 valley, Romanche valley, Great Aletsch glacier, Ferwall site) or show large standard deviations
294 (Clarée valley). Probability curves for all retained moraine mean ages in each site are plotted
295 in

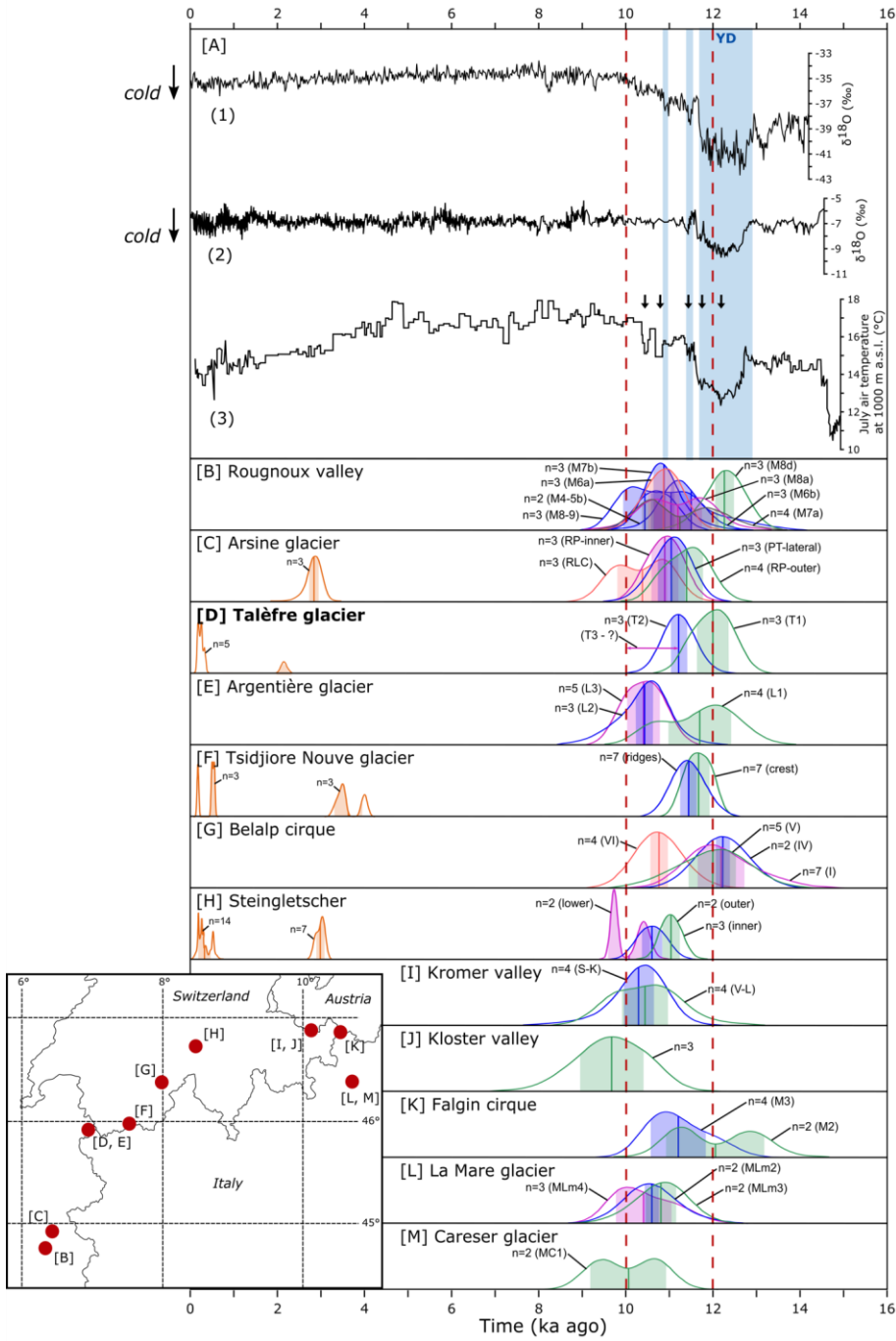


Fig. 6 in comparison with the Talèfre glacier moraine ages.

Discussion

Oscillations of Talèfre glacier since the Younger Dryas

According to the exposure ages of the two bedrock samples, the “Jardin de Talèfre” deglaciation started at ~ 12.4 ka, i.e. during the YD period, if a continuous exposure scenario is assumed.

Alternatively, the duration of ~ 12.4 ka could be composed of several exposure periods, e.g. a few hundred years of ice-free conditions during the warmer Bølling/Allerød ($\sim 14.7 - 12.9$ ka; Lotter et al., 2000; Rasmussen et al., 2006) and subsequent burial by the re-advancing glacier at the beginning of the YD. However, the only slightly younger mean age of moraine T1 (12.0 ± 0.4 ka) implies that Jardin de Talèfre was deglaciated during the YD and the central rock islet has remained ice-free since that time. The mean ages of moraines T1 and T2 are stratigraphically consistent (12.0 ± 0.4 ka and 11.2 ± 0.2 ka) and coincide with the YD/EH transition. We propose that the T3 moraine was deposited during the EH, as its morphology is very similar to T1 and T2 moraines. This suggests that the glacier underwent at least three advances or stillstands after the beginning of its retreat ~ 12.4 ka ago until the EH.

Four ~~out~~ of the five ages acquired from moraine T4 ~~are dated between~~ span from 0.18 ± 0.02 ka ~~to and~~ 0.33 ± 0.03 ka, with a mean age of 0.25 ± 0.06 years. These results indicate that the moraine was last overtopped at the end of the LIA, when several closely-spaced advances occurred. One out of the five samples of T4 is ~~dated to~~ significantly older, 2.12 ± 0.07 years (JDT-16-3). This older age can be either explained by isotope inheritance from a previous exposure duration or by accretion phases of this massive moraine that pre-dated the deposition of the LIA boulders. Such advances prior to the LIA have been reported for other glaciers in

Commenté [MLR11]: Un 'âge' ne peut pas être 'daté'...

Mis en forme : Barré

320 the French Alps: between ~3.5 ka and 0.7 ka at Mer de Glace (Le Roy et al., 2015) and ~2.1
321 ka at Argentière glacier (Le Roy, 2012) and in the Ecrins-Pelvoux massif (Le Roy et al., 2017).
322 However, our data do not allow us to decide which of the two hypotheses is more likely.

323 Fig. 5 ~~visualizes-shows~~ the large YD/EH and LIA extents of Talèfre glacier in comparison to
324 that of 2008 C.E. During the YD/EH and the LIA, the glacier is still connected with the Mer de
325 Glace, and the LIA extent is only slightly smaller than that of the YD/EH, while in 2008 C.E.
326 the glacier size is significantly reduced.

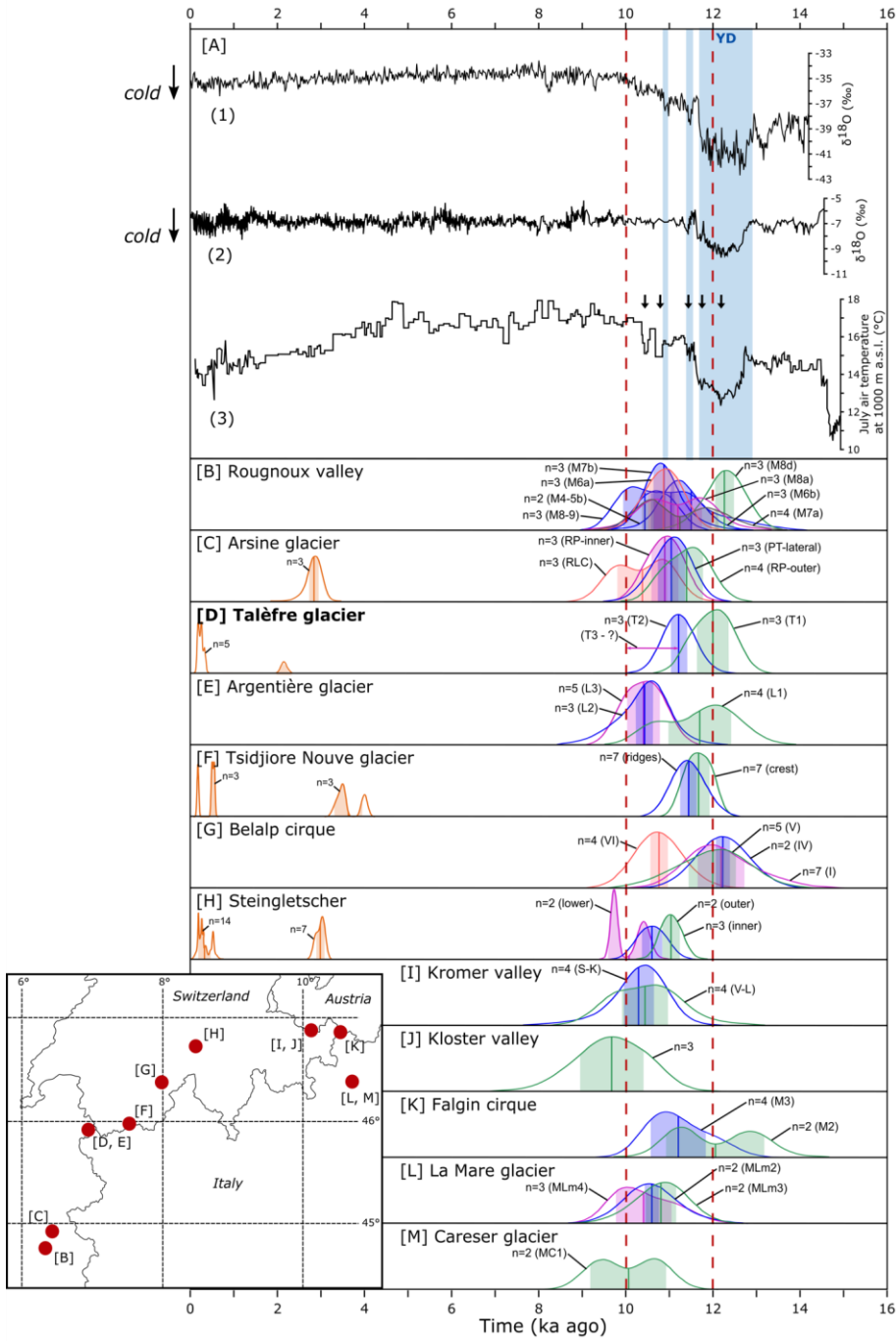
327 We do not have any evidence of glacier advances between the EH and the Late Holocene, which
328 is consistent with a warmer and dryer climate, and thus unfavorable for glacier growth in the
329 Alps, during this period (Ivy-Ochs et al., 2009). Therefore, we assume that Talèfre glacier was
330 smaller than its LIA extent during this period.

331

332 *Comparison with other Alpine glacier chronologies*

333 The YD/Holocene chronology of Talèfre glacier is very similar to the one recently established
334 at the nearby Argentière glacier (Protin et al., 2019). A similar set of bedrock surfaces (~2450m
335 a.s.l.) and five lateral moraines (~2400 - 2150m a.s.l.), dated by in situ cosmogenic ¹⁰Be to
336 between ~11.7 ka and ~10.4 ka, provide evidence of deglaciation at the end of the YD and at
337 least five glacier re-advances or stillstands during the YD/EH transition. When comparing these

338 two age sets (



340 ~~Fig. 6~~ Fig. 6 [D] and [E]), it appears that the ages of the two outermost moraines of both glaciers are
 341 undistinguishable within uncertainties, and that both glaciers oscillated several times during the
 342 YD/EH transition. In this comparison, it must be kept in mind that T3 moraine of Talèfre glacier
 343 could not be ~~dated, but~~ dated but seems to be only slightly younger than T1 and T2 moraines (section
 344 “Moraine and bedrock exposure ages”); ~~and~~ and might therefore be similar to the innermost EH
 345 ridge of Argentièrè glacier dated to 10.4 ± 0.2 ka. These moraines of Talèfre and Argentièrè
 346 glaciers thus probably represent quasi-synchronous, successive glacier stillstands within the
 347 dynamic YD/EH retreat from their larger early-YD extents.
 348 Moraines at multiple other locations across the Alps have previously been assigned to the
 349 YD/EH transition based on ^{10}Be dating. Eleven of them were selected here, based on their data
 350 quality (see section “Results”), together with our new Talèfre chronology for this regional
 351 compilation. They are geographically distributed across the European Alps (France,
 352 Switzerland, Italy and Austria), situated between longitudes $\sim 6.5^\circ\text{E}$ and 10°E and latitudes
 353 45.5°N and 47°N (Fig. 6). All of these twelve moraine chronologies indicate deposition of at
 354 least one moraine between ~ 12 and ~ 10 ka ago, *i.e.* during the YD/EH transition (Fig. 6).
 355 Further, at most sites, there is evidence of deposition of multiple lateral and/or latero-frontal
 356 moraines during this period. Successive moraines are located quite close to each other and in
 357 proximity to the LIA moraines, suggesting only slightly smaller glacier extents during the LIA
 358 than during the YD/EH compared to today’s reduced glacier sizes like at Talèfre glacier (Fig.
 359 5). The highest spatial spread is found at Arsine glacier displaying YD/EH frontal moraines
 360 that are located about 1 km downstream of the LIA moraines ([Schimmelpfennig et al., 2019;](#)
 361 [Le Roy et al., in prep](#)). At several other sites in the Alps, lateral YD/EH moraines exist within
 362 $< 300\text{m}$ -distance from lateral LIA moraines (Hofmann et al., 2019; Moran et al., 2016;
 363 Schimmelpfennig et al., ~~2019,~~ 2014, 2012).

Commenté [MOU12]: And/or Schimmelpfennig et al., 2019
 (poster)

364 Thus, based on the consistency of the ^{10}Be cosmogenic exposure ages, we show here that
365 millennial-scale synchronous glacier fluctuations occurred in the European Alps, and that
366 glaciers oscillated multiple times at centennial or sub-centennial scale superposed on a general
367 retreat trend during the 12-10 ka period. However, based on the available datasets it is not
368 possible to temporally correlate specific moraines between sites or to give evidence of a decadal
369 or centennial-scale synchronicity of glacier dynamics within the ~12-10 ka period, because of
370 (i) the analytical and geomorphic uncertainties related to the dating method; (ii) the probably
371 incomplete preservation of the moraine records or no deposition of the moraine; (iii) undated
372 ridges within the investigated moraine sequences at several sites.

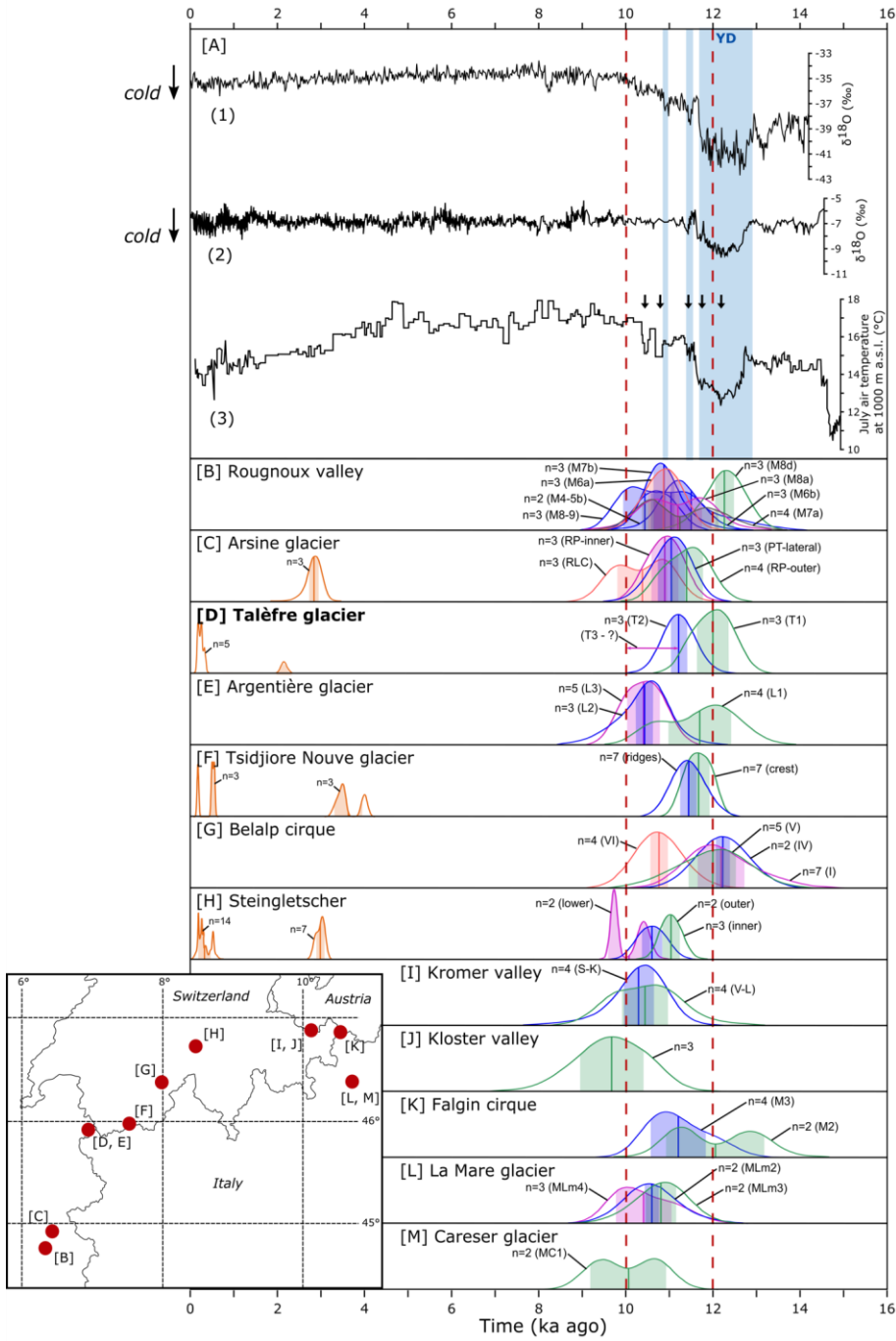
373 For the sites where ELA depressions between the YD/EH transition and the LIA have been
374 calculated using the Accumulation Area Ratio method with a ratio of 0.67 (Table S1), no
375 significant correlations between moraine ages and ELA depressions are observed (Fig. S1). In
376 fact, the large range of ELA depressions supports the findings by Boxleitner et al. (2019) that
377 indicate ELA depressions should not be used to temporally correlate moraines from different
378 valleys, as previously proposed by Maisch (1981). This reflects the fact that ELA variations of
379 individual glaciers might be significantly influenced by local precipitation amounts and local
380 glacier morphology, as well as the limitations of the AAR method (e.g. Boxleitner et al., 2019;
381 Reitner et al., 2016).

382

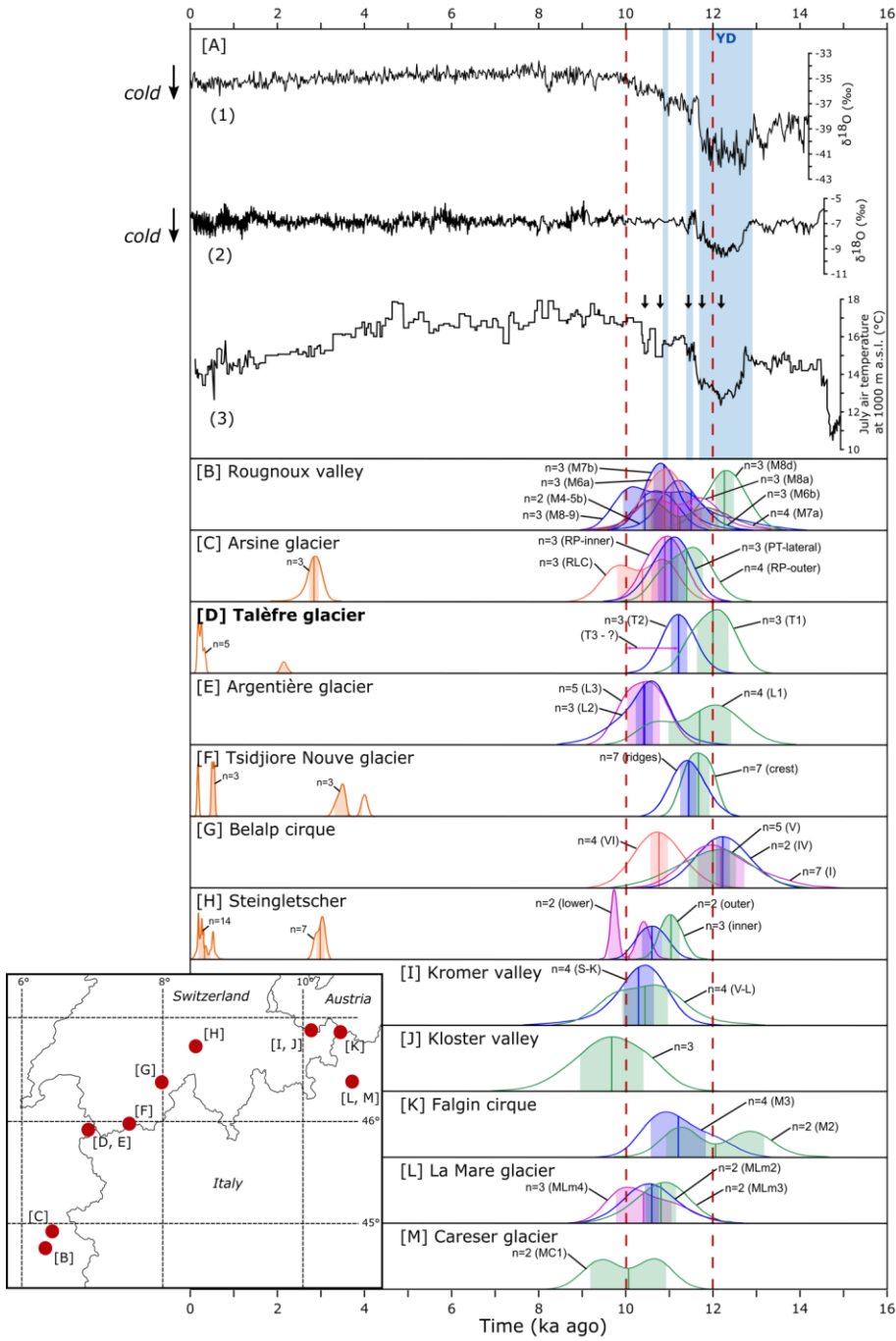
383 *Link of the Alpine glacier oscillations with regional climate*

384 Analysis of the geographic characteristics of the 12 selected sites implies that their millennial
385 synchronicity is independent of their altitude range (at present between 1500 and 3400 m a.s.l.),
386 orientation (all directions) and size (0.3 to 14 km²) (Fig. S1). In the absence of common
387 topographic characteristics of the glaciers, the only process to explain the millennial-scale
388 synchronous fluctuations of independent ice masses fluctuations across the European Alps is a

389 regional climatic signal that prevailed over local factors. Therefore, we here compare the
390 moraine chronologies with regional - and high-latitude - independent climate proxy records in
391 an effort to elucidate the spatial reach of the climatic evolution underlying the quasi-
392 simultaneous glacier oscillations across the European Alps within their dynamic retreat.
393 Glaciers are sensitive to a variety of climatic factors, but the main driver for large-scale, long-
394 term glacier fluctuations in the mid- and high latitudes is the impact of summer temperature
395 variations (e.g. Oerlemans, 2005; Solomina et al., 2015) on which we therefore
396 ~~focussed~~focused. In addition, over the last century, annual mass balance of Alpine glaciers have
397 been shown to be mainly driven by summer melting (Huss et al., 2010). In the Alpine and pre-
398 Alpine region, evidence of a temperature minimum in the middle of the YD and several distinct
399 cold events during a general warming trend within the 12-10 ka period comes from various
400 high-resolution paleorecords that reflect variations either in July air temperatures (based on
401 chironomid-inferred records from lakes in eastern France and the northern and central Swiss
402 Alps; Heiri et al., 2015 -



404 [Fig. 6](#) [A3]) or in mean annual temperatures, based on stable isotope measurements in
405 stalagmites (Affolter et al., 2019 -

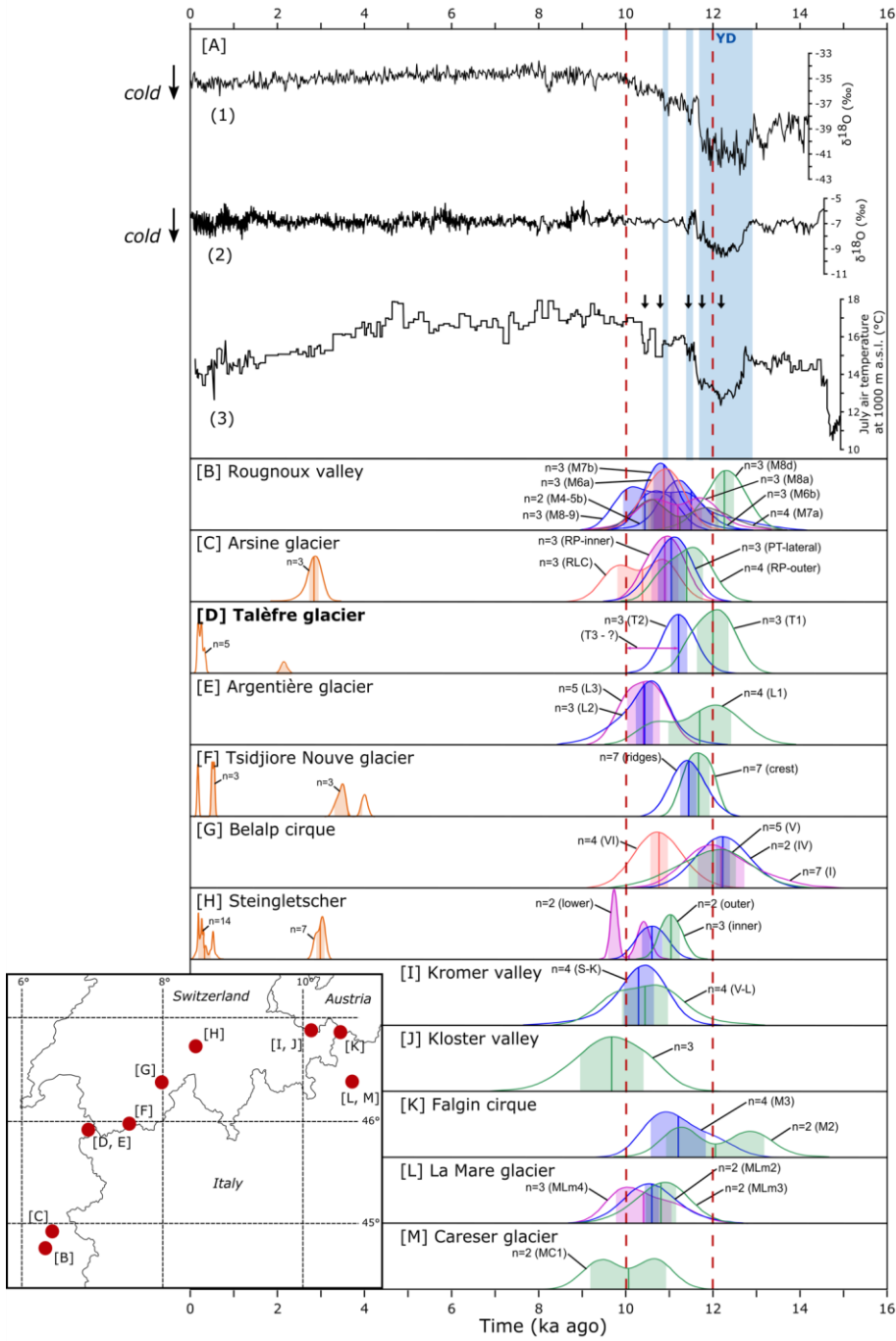


407 ~~Fig. 6~~ Fig. 6 [A2]; Wurth et al., 2004) and biogenically precipitated carbonates in lake sediments
408 (Schwander et al., 2000). These decadal to centennial cold peaks seem to have amplitudes in
409 the order of $\sim 0.5^{\circ}\text{C}$, i.e. similar to the multidecadal fluctuations that drove the succession of
410 LIA moraines in the Alps (Oerlemans, 2005). Regional cold peaks could therefore be sufficient
411 to lead to the YD/EH succession of glacial culminations or still-stands during the general
412 deglaciation observed in the Alps. In this case, it is most likely that decadal to centennial glacier
413 oscillations occurred quasi-simultaneously across the Alps.

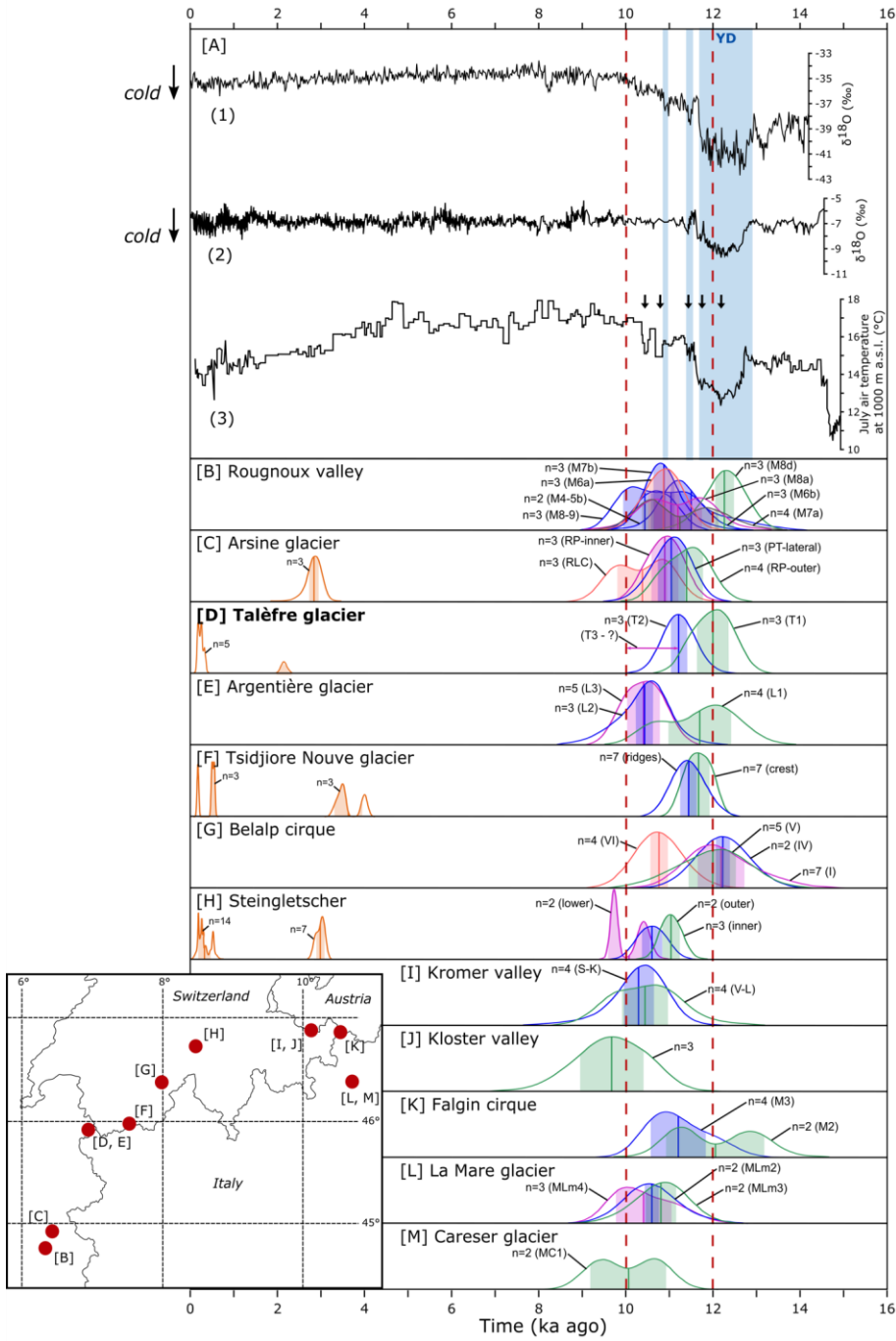
414

415 *Link of the Alpine glacier extents with seasonality*

416 It is remarkable that several glaciers around 12 ka ago, i.e. at the end of the YD, were only
417 slightly larger than during the EH. This is the case for Rougnoux valley, Arsine, Talèfre,
418 Argentièrre, Tsidjiore Nouve, Belalp and Falgin Cirque glaciers, where the ages of the outermost
419 moraine fall into the YD or their uncertainties overlap with it (green probability curves in



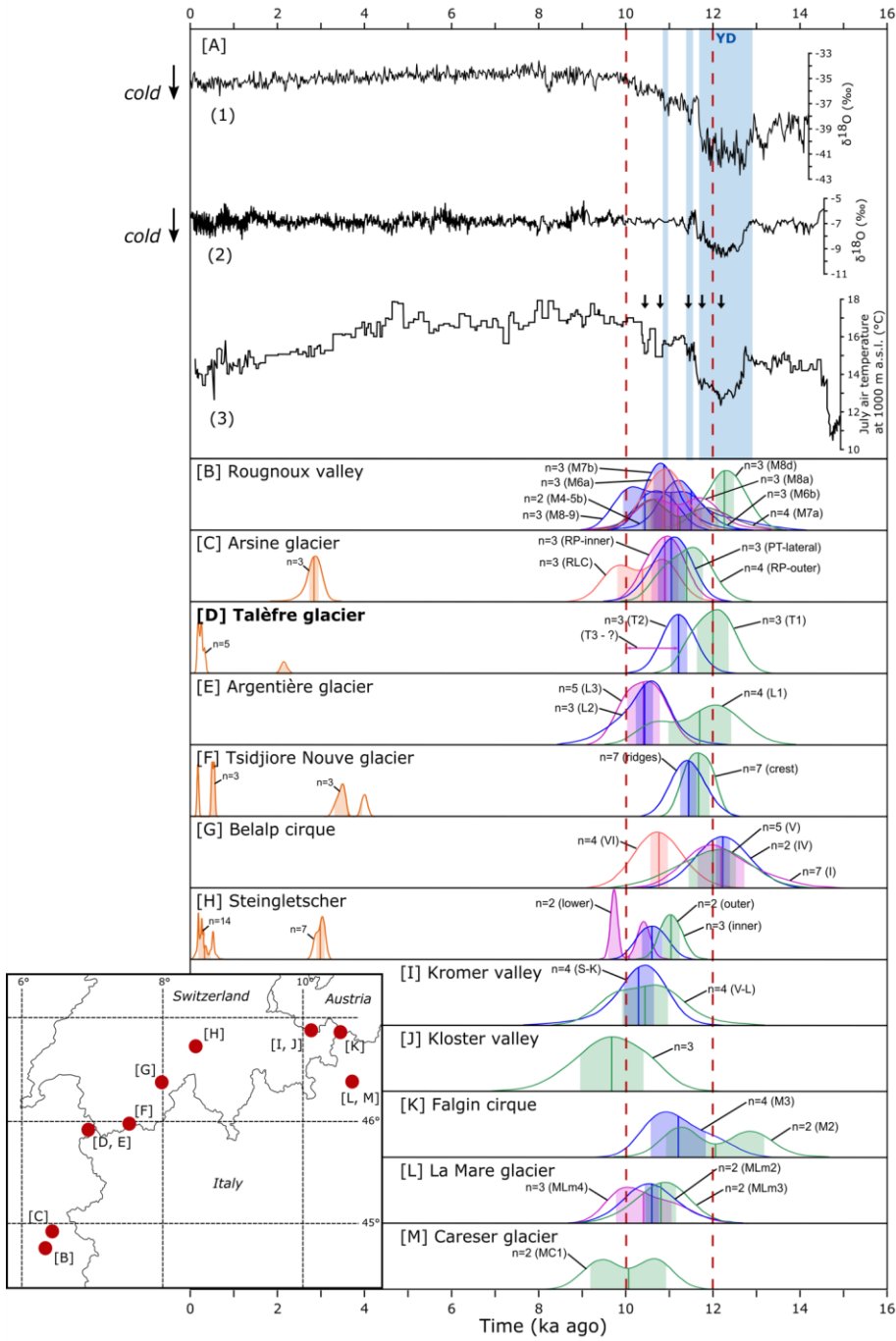
421 [Fig. 6](#) and the ages of the innermost moraine fall into the EH. This small difference between
422 late YD and EH glacier extents seems inconsistent with the drastic YD temperature cooling and
423 abrupt mean annual temperature increase that characterizes the boundary between these two
424 periods (



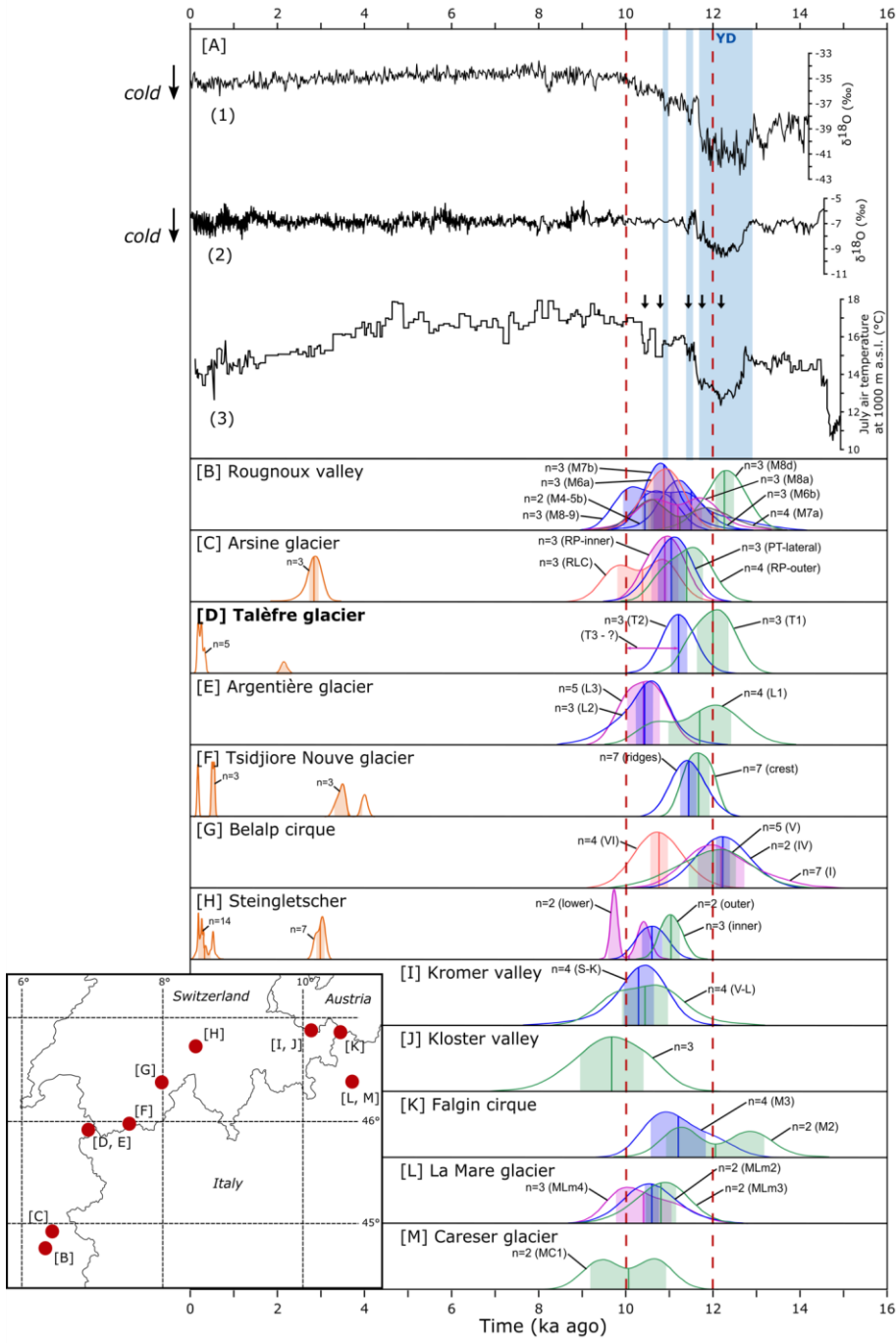
426 ~~Fig. 6~~ Fig-6 [A]). A linear relationship between oxygen isotope record and temperature would suggest
427 that the coldest YD temperatures of the Greenland sites were only slightly higher than those of
428 the Last Glacial Maximum (e.g. Rasmussen et al., 2008) when Alpine glaciers reached until the
429 Alpine foreland (Ivy-Ochs et al., 2008). Much larger glacier extents might therefore be expected
430 during and at the end of the ~1 ka lasting YD, especially compared to the EH and LIA. In
431 addition, the ^{10}Be bedrock ages from outboard of the oldest dated moraines of Talèfre and
432 Argentièrre glaciers suggest that these glaciers have been retreating prior to the deposition of
433 their respective late YD moraine. These results are in line with ^{10}Be -based glacier chronologies
434 from Greenland, also providing evidence of ice mass downwasting throughout the YD, which
435 lasted until the EH (Rainsley et al., 2018 and references therein).

436 The apparent mismatch between the glacier proxy records and the mean annual temperature
437 climate proxies could be due to a difference in seasonality between the YD and the EH. This
438 concept of seasonality was first proposed by Denton et al. (2005) to explain the discord between
439 the drastic change of the mean annual temperature observed in Greenland ice cores and the
440 slight snowline change of glaciers in Greenland and Europe during the YD and EH. The YD,
441 as well as other abrupt climate changes, has been qualified as a winter phenomenon (Denton et
442 al., 2005), meaning that the considerable annual temperature switches observed in paleoclimate
443 records from Europe and Greenland are mainly due to changes in winter temperature, while
444 summer temperature did only undergo minor changes (Buizert et al., 2014; Renssen and Isarin,
445 2001; Schenk et al., 2018).

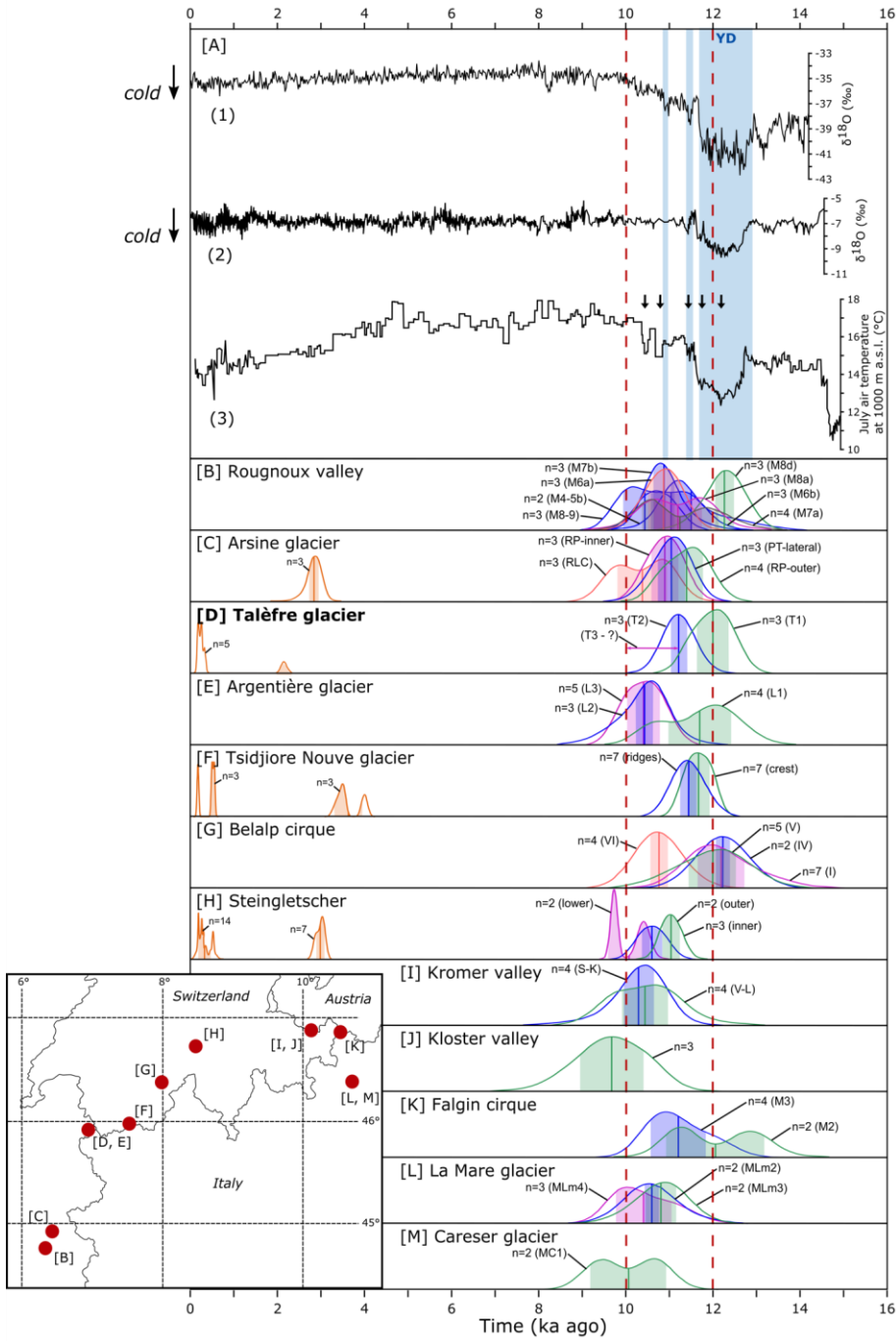
446 In the Alpine region, a decrease of the seasonality between the YD and EH is supported by the
447 difference of mean annual and summer warming estimated from the above-mentioned recent
448 independent proxy studies (



450 [Fig. 6](#) [A2, 3]; Affolter et al., 2019; Heiri et al., 2015). The stable isotope measurements in
451 speleothems suggest an increase of the mean annual temperature of $\sim 5.4^{\circ}\text{C}$ at the YD/EH
452 transition (

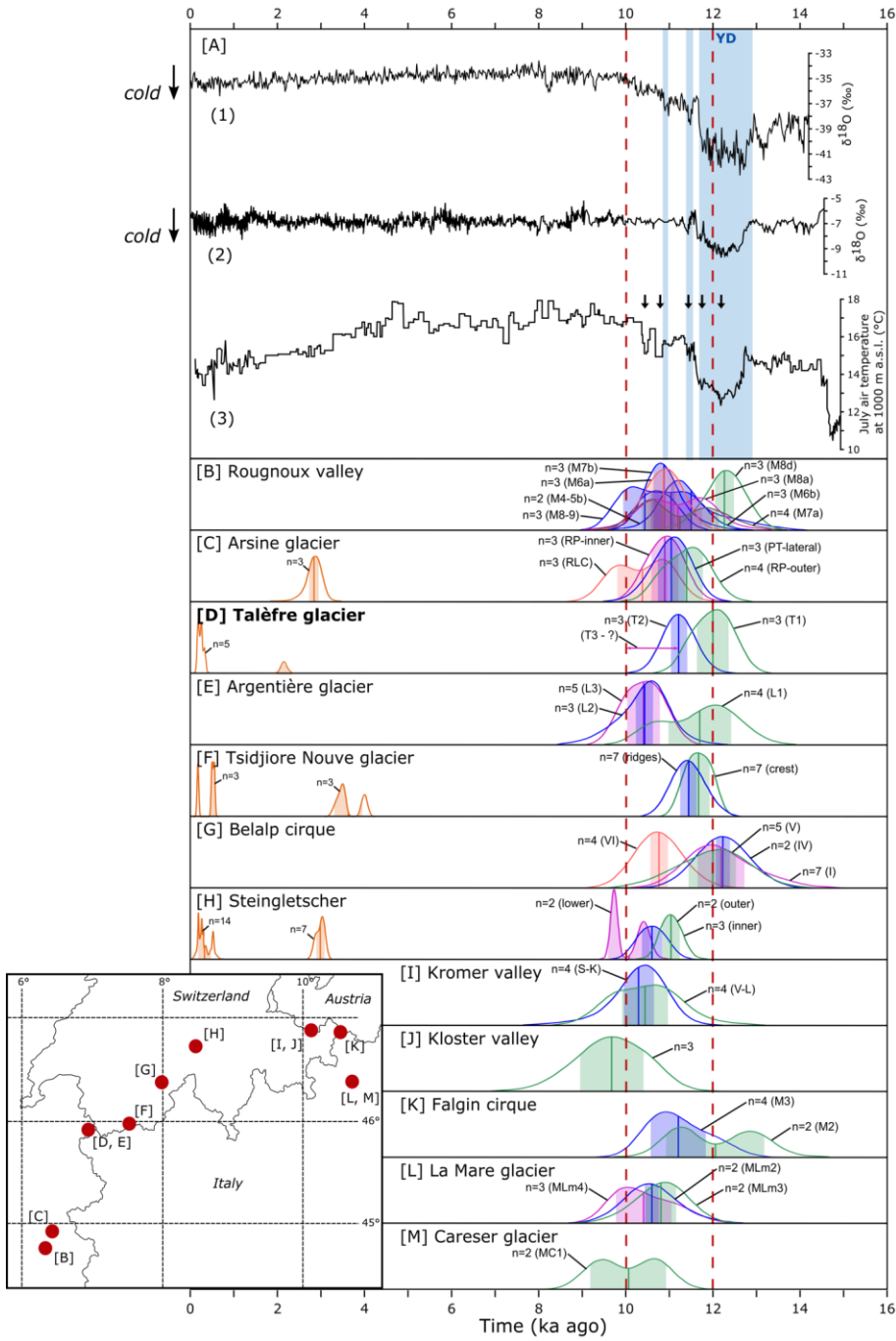


454 [Fig. 6](#) [A2]; Affolter et al., 2019), while a summer temperature increase of only $\sim 2.7^{\circ}\text{C}$ is
455 inferred from the chironomid-based lake records (

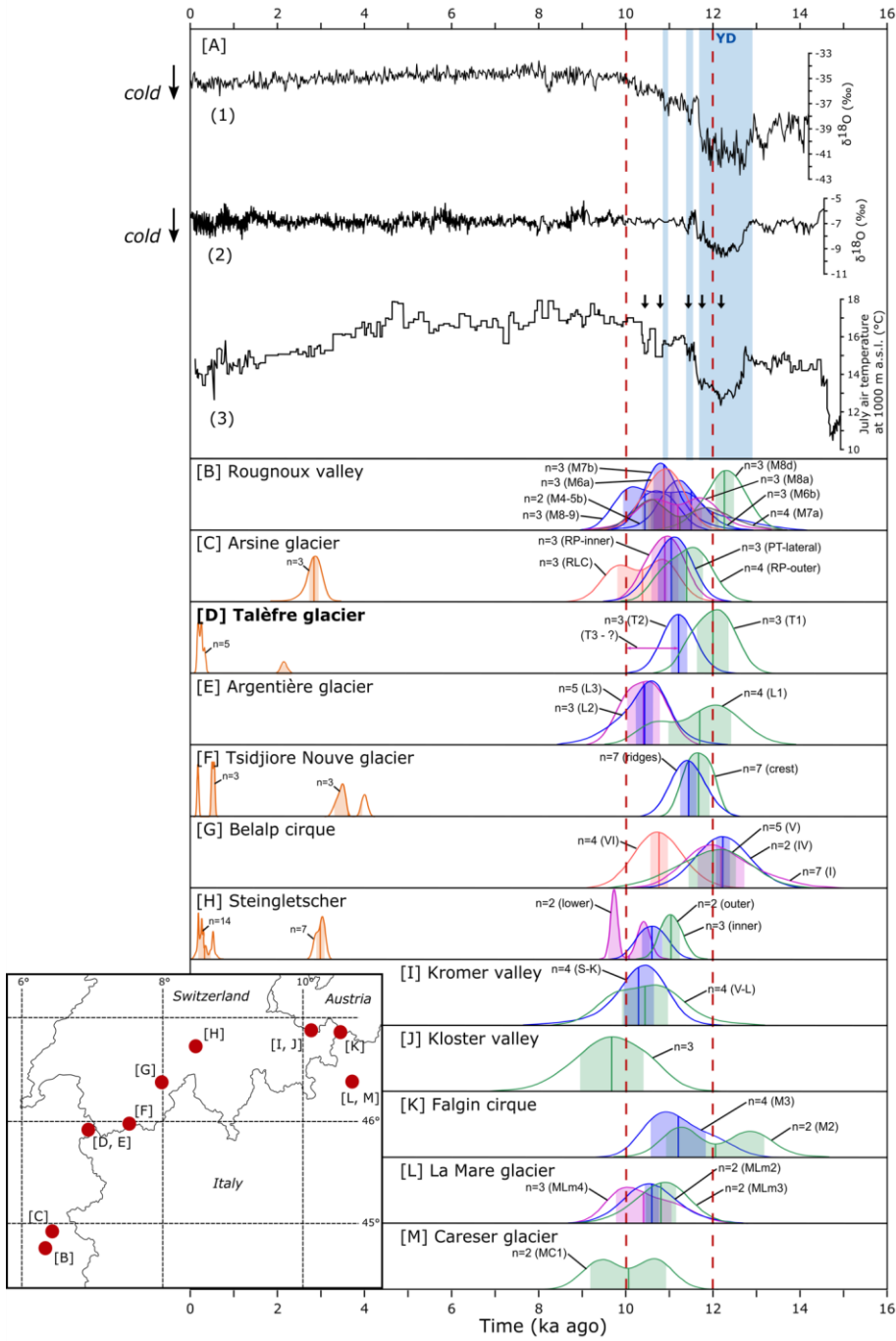


457 ~~Fig. 6~~ Fig. 6 [A3]; Heiri et al., 2015). This difference between annual and summer temperature could
458 be explained by a greater winter warming of more than 7°C if winter and summer periods are
459 assumed of equal duration. Furthermore, while the mean temperature ~~increase~~ increases in Greenland
460 occurred in less than one hundred years (

Commenté [MOU13]: Moi, j'aurais laisser increase



462 [Fig. 6](#) [A1]; Rasmussen et al., 2006), the European records indicate a more gradual warming
463 distributed over several hundred years (

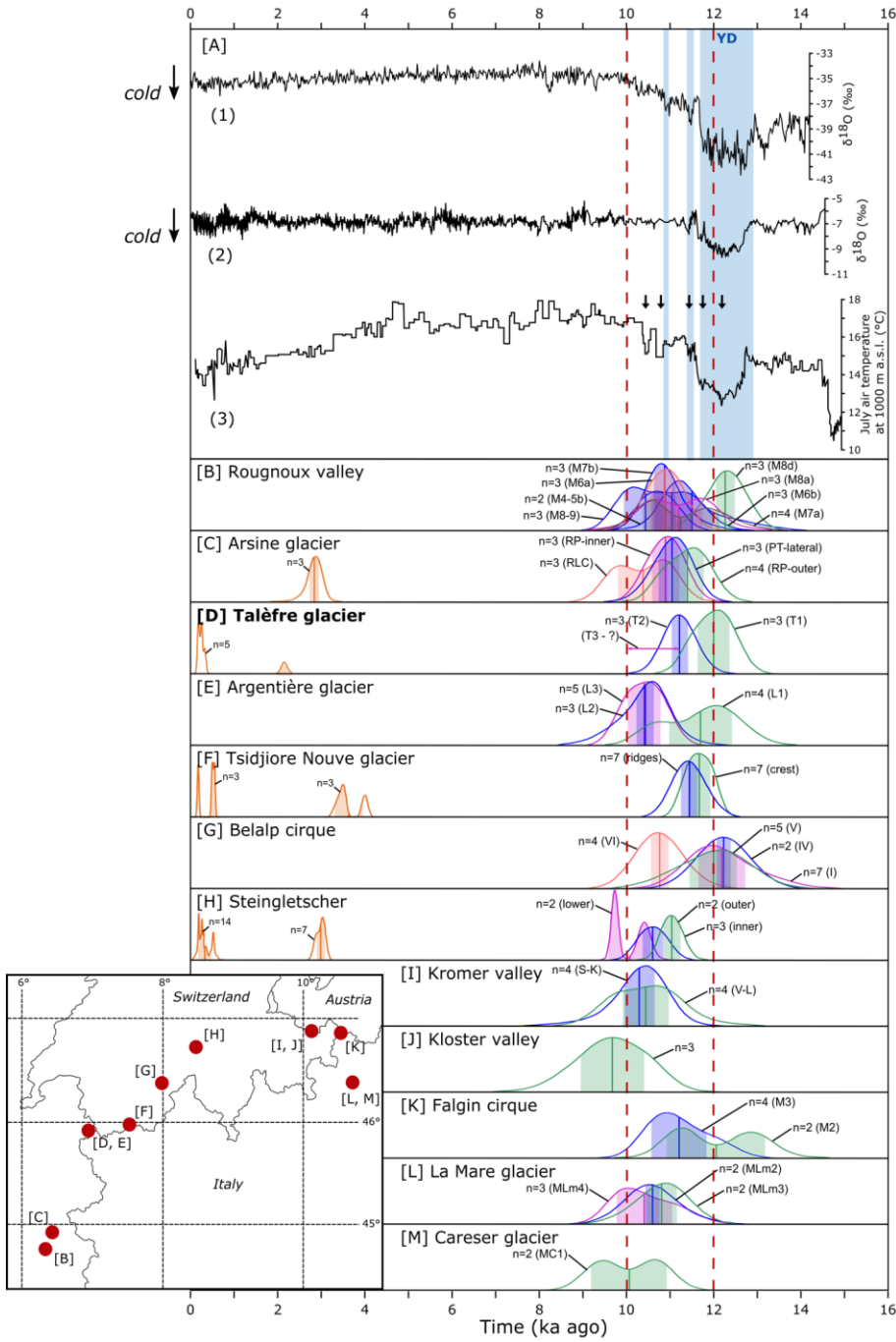


465 ~~Fig. 6~~ Fig. 6 [A2, 3]). Our ~~result~~ observations support this concept, i.e. relatively mild YD summer temperatures
466 could explain why the glaciers in the Alps did not undergo a much more pronounced retreat at
467 the YD/EH transition, but glaciers retreated gradually from their only slightly larger YD
468 extents.

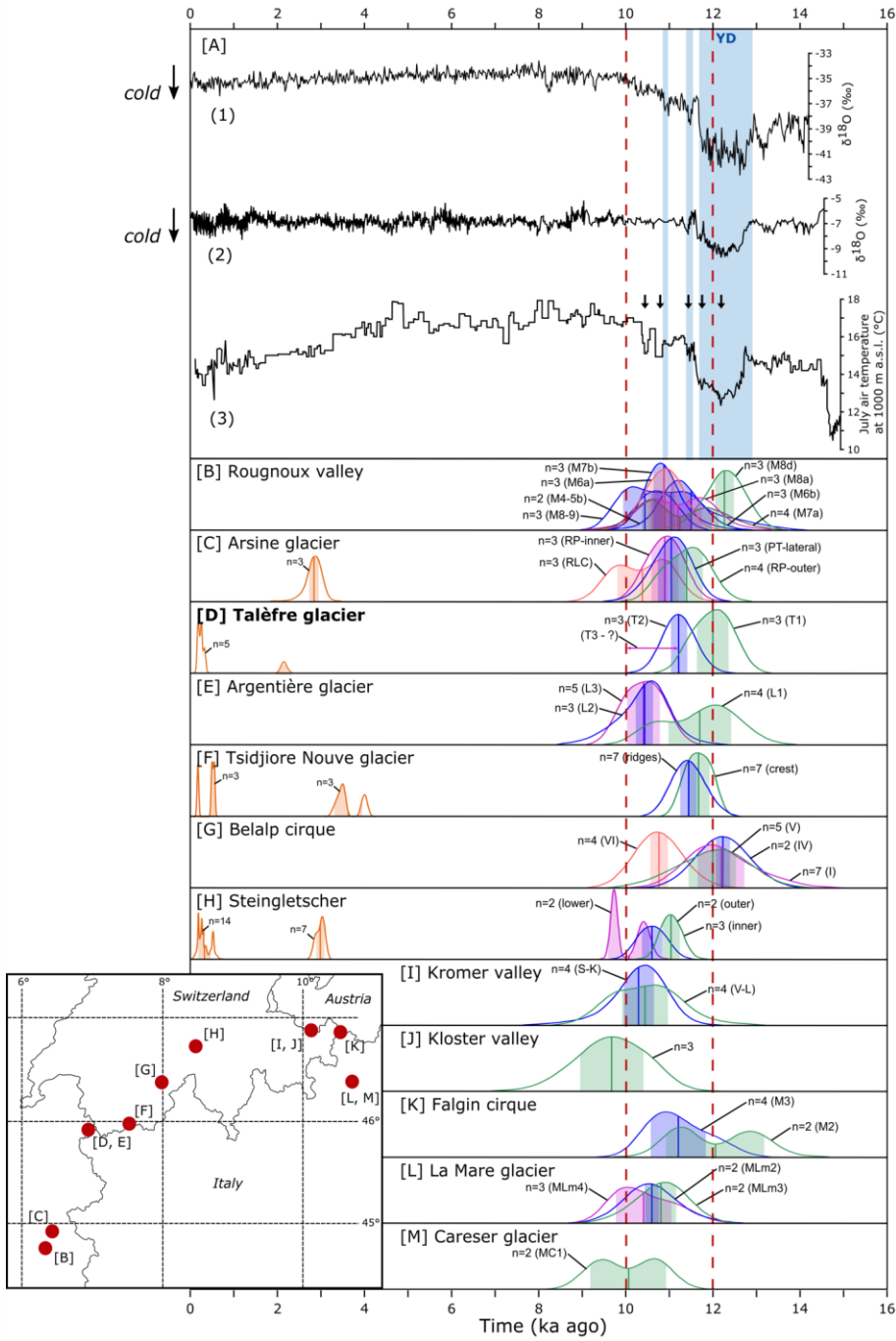
469

470 *Link of the Alpine glacier oscillations with high latitude climate*

471 The clear correlation of high-resolution proxy records from the Alps and the Alpine foreland (



473 [Fig. 6](#) [A2, 3]; Affolter et al., 2019; Heiri et al., 2015) with the pattern of oxygen isotope
474 variations in Greenland ice cores (e.g. Rasmussen et al., 2006;



476 ~~Fig. 6~~ Fig. 6 [A1]) strongly suggests a climatic link of the Alpine region with the northern high
477 latitudes. In this context, a recent study by Young et al. (2020) provides evidence of a
478 succession of re-advances or stillstands of ~~a~~ mountain glaciers, the Laurentide Ice Sheet and
479 Greenland Ice Sheet in the Baffin Bay region at ~11.8-11.6 ka, ~10.4 ka, ~9.3 ka. The striking
480 similarity of these moraine-based chronologies from and near western Greenland with those
481 from the European Alps provide further evidence of a teleconnection between both regions at
482 that time and that the observed glacier fluctuations were due to a common climate evolution on
483 extra-regional, maybe even hemispheric scale.

484 The question arises which large-scale climate mechanisms led to this teleconnection and the
485 contrasted seasonality imprinted in the above-discussed summer temperature and mean annual
486 temperature records. The abrupt onset of the YD cooling and the cold peaks of the Late YD and
487 EH in the high latitudes are thought to have been triggered by freshwater input from the
488 Laurentide Ice Sheet into the North Atlantic (Jennings et al., 2015) leading to a reduction of the
489 Atlantic Meridional Ocean Circulation (AMOC) (Renssen et al., 2015). The related
490 development of expanded wintertime sea ice in the North Atlantic shifted the westerlies south
491 leading to wind-transported cool temperatures to Europe (Bakke et al., 2009; Brauer et al.,
492 2008), and therefore to the Alps. During the second half of the YD, brief sea-ice breakups were
493 led by incursions of the Atlantic circulation and were associated with a northwards migration
494 of the polar front and westerly storm tracks (Bakke et al., 2009) until the system abruptly
495 switched to the interglacial state at the onset of the Holocene (Rasmussen et al., 2006). The
496 signature of these climatic mechanisms is markedly imprinted in the abrupt variations of the
497 mean annual temperature proxy records, but to a lesser degree in the glacier mass balance
498 fluctuations. Robust evidence of drastic glacier expansion in the Alps and the high latitudes in
499 relation with the strong annual cooling observed in the first part of the YD is rare so far. Early
500 to mid-YD moraines are preserved at a few sites [in the Alps and at other sites in the North](#)

501 [Atlantic region](#) (e.g. Belalp and Aletsch Glacier, Kelly et al., 2004; Schindelwig et al., 2012;
502 Julier Pass, Ivy-Ochs, 2015; Alaska, Young et al., 2019; Norway, Wittmeier et al., 2020), but
503 the corresponding glacier extents were relatively modest compared to significant annual
504 temperature decrease. In addition, the deglaciation during the YD/EH transition was rather
505 gradual and punctuated by closely-spaced short-lived re-advances or stillstands. This could be
506 explained by several mechanisms. Sea ice expansion occurs predominantly in winter and might
507 therefore not directly result in a summer temperature decrease. In addition, the drastic YD
508 cooling recorded by the mean annual temperature proxies was enhanced by an increased
509 strength of wind only during autumn, winter and spring, which transported cold air from the
510 ice-covered North Atlantic region and led to cool and dry winters in Europe (Brauer et al.,
511 2008). This phenomenon did not occur during summer due to atmospheric blocking of the cold
512 westerlies over Fennoscandia leading to warm summers during the YD (Schenk et al., 2018).
513 Therefore, and because snowfall was reduced during the dry winters of the cold periods, greater
514 glacier expansion did not occur at many sites. Nevertheless, summers were very short, probably
515 because winter sea ice expansion lasted for a long period of the year, leading to a reduced
516 glacier melt season (Young et al., 2020). This might explain why glaciers responded with
517 successive glacier advances or stillstands to these dynamic changes in seasonality both in high
518 latitudes and Europe.

519

520 Conclusion

521 Our new chronology based on 14^{10}Be cosmogenic exposure ages on moraine and bedrock from
522 the “Jardin de Talèfre” suggests that Talèfre glacier retreated from its YD position starting
523 ~12.4 ka ago. This retreat was interrupted by several episodes of stillstands before a major
524 retreat during the EH. No evidence of re-advances before the Late Holocene is preserved, with
525 the most remarkable advance during the LIA, which was only slightly less extensive than the

526 late YD and EH glacier extents at our [high-elevation site](#). This behavior is very similar to that
527 of the nearby Argentière glacier. The comparison of the YD/EH transition moraine chronology
528 of Talèfre glacier with those of eleven other Alpine glaciers scattered throughout the Alps
529 suggests a period of roughly synchronous glacial behavior across the Alps between 12 and 10
530 ka ago. Several glaciers deposited multiple moraines, which attest to regional-scale stillstands
531 or re-advances during the deglaciation. Similarities with paleotemperature records from the
532 Alpine region as well as with glacial culminations and temperature records from Greenland
533 strongly suggest not only a regional-wide common climate driver, but also a teleconnection
534 with the high latitudes, thus reinforcing the hypothesis postulated in earlier studies of a link
535 between YD and EH Alpine glacier fluctuations and Greenland climate change. However, the
536 relatively small amplitude of the YD glacier extents compared to the Holocene glacier extents
537 is inconsistent with the large and abrupt temperature shifts imprinted in mean annual proxy
538 records in both regions. We suggest that this inconsistency is due to a pronounced change in
539 seasonality, with YD winters cold and dry and YD summers only slightly cooler than those of
540 the EH. This seasonality difference controlled YD glacier extents and led to YD glaciers only
541 slightly larger than during the EH.

542

543 Acknowledgements

544 This study is part of ANR 14-CE03-0006 *VIP Mont-Blanc*. We thank Laëtitia Léanni
545 (CEREGE) for support during chemistry and Jean Hanley and Roseanne Schwartz (LDEO,
546 Columbia University) for advices on sample chemistry and Joerg Schaefer (LDEO, Columbia
547 University) for discussion. The ASTER AMS national facility (CEREGE) is supported by the
548 INSU/CNRS, the ANR through the “projet thématiques d’excellence” program for the
549 “Equipements d’excellence” ASTER-CEREGE action and IRD. An earlier version of this
550 manuscript greatly benefitted from constructive comments by Benjamin Chandler. We thank

551 Marie Chenet and an anonymous reviewer whose relevant comments have helped to improve
552 this manuscript.

553

554 Author contributions

555 JLM, IS, JFB and BP acquired the funding for the project leading to this publication. MP, JLM,
556 JFB, BP and LM conducted the fieldwork. MP carried out the laboratory work. ASTER Team
557 realized the AMS measurements. MP, IS, ~~and JLM~~ and MLR did the data analysis and prepared
558 the original draft of the manuscript and all co-authors contributed the final draft of the
559 manuscript.

560

561 Data availability

562 The data that support the findings of this study are available from the corresponding author
563 upon reasonable request.

564

565 References

566 Affolter, S., Häuselmann, A., Fleitmann, D., Edwards, R.L., Cheng, H., Leuenberger, M., 2019:
567 Central Europe temperature constrained by speleothem fluid inclusion water isotopes over the
568 past 14,000 years. *Science Advances* 5, eaav3809.

569 André, M., 2002: Rates of postglacial rock weathering on glacially scoured outcrops (abisko-
570 riksgåränsen area, 68°N): *Geografiska Annaler: Series A, Physical Geography* 84, 139–150.

571 Arnold, M., Merchel, S., Bourlès, D.L., Braucher, R., Benedetti, L., Finkel, R.C., Aumaître, G.,
572 Gottdang, A., Klein, M., 2010: The French accelerator mass spectrometry facility ASTER:
573 Improved performance and developments. *Nuclear Instruments and Methods in Physics*
574 *Research Section B: Beam Interactions with Materials and Atoms* 268, 1954–1959.

575 Bakke, J., Lie, Ø., Heegaard, E., Dokken, T., Haug, G.H., Birks, H.H., Dulski, P., Nilsen, T.,

Commenté [MLR14]: Comme il faut faire apparaitre la
tache de tous les co-auteurs à cet endroit je suggère que tu me
mettes là...

- 576 2009: Rapid oceanic and atmospheric changes during the Younger Dryas cold period. *Nature*
577 *Geoscience* 2, 202–205.
- 578 Balco, G., 2017: Production rate calculations for cosmic-ray-muon-produced ^{10}Be and ^{26}Al
579 benchmarked against geological calibration data. *Quaternary Geochronology* 39, 150–173.
- 580 Balco, G., Briner, J., Finkel, R.C., Rayburn, J.A., Ridge, J.C., Schaefer, J.M., 2009: Regional
581 beryllium-10 production rate calibration for late-glacial northeastern North America.
582 *Quaternary Geochronology* 4, 93–107.
- 583 Balco, G., Stone, J.O., Lifton, N.A., Dunai, T.J., 2008: A complete and easily accessible means
584 of calculating surface exposure ages or erosion rates from ^{10}Be and ^{26}Al measurements.
585 *Quaternary Geochronology* 3, 174–195.
- 586 Baroni, C., Casale, S., Salvatore, M.C., Ivy-Ochs, S., Christl, M., Carturan, L., Seppi, R.,
587 Carton, A., 2017: Double response of glaciers in the Upper Peio Valley (Rhaetian Alps, Italy)
588 to the Younger Dryas climatic deterioration. *Boreas* 46, 783–798.
- 589 Borchers, B., Marrero, S., Balco, G., Caffee, M., Goehring, B., Lifton, N., Nishiizumi, K.,
590 Phillips, F., Schaefer, J., Stone, J., 2016: Geological calibration of spallation production rates
591 in the CRONUS-Earth project. *Quaternary Geochronology* 31, 188–198.
- 592 Boxleitner, M., Ivy-Ochs, S., Egli, M., Brandova, D., Christl, M., Maisch, M., 2019: Lateglacial
593 and Early Holocene glacier stages - New dating evidence from the Meiental in central
594 Switzerland. *Geomorphology* 340, 15–31.
- 595 Braucher, R., Guillou, V., Bourlès, D.L., Arnold, M., Aumaître, G., Keddadouche, K., Nottoli,
596 E., 2015: Preparation of ASTER in-house $^{10}\text{Be}/^{9}\text{Be}$ standard solutions. *Nuclear Instruments*
597 *and Methods in Physics Research Section B: Beam Interactions with Materials and Atoms* 361,
598 335–340.
- 599 Brauer, A., Haug, G.H., Dulski, P., Sigman, D.M., Negendank, J.F.W., 2008: An abrupt wind
600 shift in western Europe at the onset of the Younger Dryas cold period. *Nature Geoscience* 1,

- 601 520–523.
- 602 Braumann, S.M., Schaefer, J.M., Neuhuber, S.M., Reitner, J.M., Lüthgens, C., Fiebig, M.,
603 2020: Holocene glacier change in the Silvretta Massif (Austrian Alps) constrained by a new
604 ^{10}Be chronology, historical records and modern observations. *Quaternary Science Reviews*
605 245, 106493.
- 606 Buizert, C., Gkinis, V., Severinghaus, J.P., He, F., Lecavalier, B.S., Kindler, P., Leuenberger,
607 M., Carlson, A.E., Vinther, B., Masson-Delmotte, V., White, J.W.C., Liu, Z., Otto-Bliesner, B.,
608 Brook, E.J., 2014: Greenland temperature response to climate forcing during the last
609 deglaciation. *Science* 345, 1177–1180.
- 610 Bussy, F., Hernandez, J., Raumer, J.V., 2000. Bimodal magmatism as a consequence of the
611 post-collisional readjustment of the thickened Variscan continental lithosphere (Aiguilles
612 Rouges-Mont Blanc Massifs, Western Alps). *Earth and Environmental Science Transactions*
613 *of The Royal Society of Edinburgh* 91, 221–233.
- 614 Chenet, M., Brunstein, D., Jomelli, V., Roussel, E., Rinterknecht, V., Mokadem, F., Biette, M.,
615 Robert, V., Léanni, L., 2016: ^{10}Be cosmic-ray exposure dating of moraines and rock
616 avalanches in the Upper Romanche valley (French Alps): Evidence of two glacial advances
617 during the Late Glacial/Holocene transition. *Quaternary Science Reviews* 148, 209–221.
- 618 Chmeleff, J., von Blanckenburg, F., Kossert, K., Jakob, D., 2010: Determination of the ^{10}Be
619 half-life by multicollector ICP-MS and liquid scintillation counting. *Nuclear Instruments and*
620 *Methods in Physics Research Section B: Beam Interactions with Materials and Atoms* 268,
621 192–199.
- 622 Claude, A., Ivy-Ochs, S., Kober, F., Antognini, M., Salcher, B., Kubik, P.W., 2014: The
623 Chironico landslide (Valle Leventina, southern Swiss Alps): age and evolution. *Swiss Journal*
624 *of Geosciences* 107, 273–291.
- 625 Cossart, E., Fort, M., Bourlès, D., Braucher, R., Perrier, R., Siame, L., 2012: Deglaciation

- 626 pattern during the Lateglacial/Holocene transition in the southern French Alps. Chronological
627 data and geographical reconstruction from the Clarée Valley (upper Durance catchment,
628 southeastern France). *Palaeogeography, Palaeoclimatology, Palaeoecology* 315–316, 109–
629 123.
- 630 de Decker Heftler, S., 2002: Photographier le Mont Blanc, Guerin. ed.
- 631 Denton, G., Alley, R., Comer, G., Broecker, W., 2005: The role of seasonality in abrupt climate
632 change. *Quaternary Science Reviews* 24, 1159–1182.
- 633 Fischer, M., Huss, M., Barboux, C., Hoelzle, M., 2014: The New Swiss Glacier Inventory
634 SGI2010: Relevance of Using High-Resolution Source Data in Areas Dominated by Very Small
635 Glaciers. *Arctic, Antarctic, and Alpine Research* 46, 933–945.
- 636 Gardent, M., 2014: Inventaire et retrait des glaciers dans les alpes françaises depuis la fin du
637 Petit Age Glaciaire. (PhD thesis) Université de Grenoble.
- 638 Gardent, M., Rabatel, A., Dedieu, J.-P., Deline, P., 2014: Multitemporal glacier inventory of
639 the French Alps from the late 1960s to the late 2000s. *Global and Planetary Change Glob.*
640 *Planet. Change* 120, 24–37
- 641 Heiri, O., Ilyashuk, B., Millet, L., Samartin, S., Lotter, A.F., 2015: Stacking of discontinuous
642 regional palaeoclimate records: Chironomid-based summer temperatures from the Alpine
643 region. *The Holocene* 25, 137–149.
- 644 Hofmann, F.M., 2018: Glacial history of the upper Drac Blanc catchment (Écrins massif,
645 French Alps). *E&G Quaternary Science Journal* 67, 37–40.
- 646 Hofmann, F.M., Alexanderson, H., Schoeneich, P., Mertes, J.R., Léanni, L., Aster Team
647 (Georges Aumaître, Didier L. Bourlès, Karim Keddadouche), 2019: Post-Last Glacial
648 Maximum glacier fluctuations in the southern Écrins massif (westernmost Alps): insights from
649 ¹⁰Be cosmic ray exposure dating. *Boreas* 48, 1019-1041.
- 650 Huss, M., Hock, R., Bauder, A., Funk, M., 2010: 100-year mass changes in the Swiss Alps

- 651 linked to the Atlantic Multidecadal Oscillation. *Geophysical Research Letters* 37,
652 <https://doi.org/10.1029/2010GL042616>.
- 653 Ivy-Ochs, S., 2015: Glacier variations in the European Alps at the end of the last glaciation.
654 *Cuadernos de Investigación Geográfica* 41, 295-315.
- 655 Ivy-Ochs, S., Kerschner, H., Maisch, M., Christl, M., Kubik, P.W., Schlüchter, C., 2009: Latest
656 Pleistocene and Holocene glacier variations in the European Alps. *Quaternary Science Reviews*
657 28, 2137–2149.
- 658 Ivy-Ochs, S., Kerschner, H., Reuther, A., Maisch, M., Sailer, R., Schaefer, J., Kubik, P.W.,
659 Synal, H.-A., Schluechter, C., 2006: The timing of glacier advances in the northern European
660 Alps based on surface exposure dating with cosmogenic ^{10}Be , ^{26}Al , ^{36}Cl , and ^{21}Ne . *In Situ-*
661 *Produced Cosmogenic Nuclides and Quantification of Geological Processes*, Ana María
662 Alonso-Zarza, Lawrence H. Tanner.
- 663 Ivy-Ochs, S., Kerschner, H., Reuther, A., Preusser, F., Heine, K., Maisch, M., Kubik, P.W.,
664 Schlüchter, C., 2008: Chronology of the last glacial cycle in the European Alps. *Journal of*
665 *Quaternary Science* 23, 559–573.
- 666 Jennings, A., Andrews, J., Pearce, C., Wilson, L., Ólfasdóttir, S., 2015: Detrital carbonate
667 peaks on the Labrador shelf, a 13–7ka template for freshwater forcing from the Hudson Strait
668 outlet of the Laurentide Ice Sheet into the subpolar gyre. *Quaternary Science Reviews* 107, 62–
669 80.
- 670 Joly, D., Berger, A., Buoncristiani, J.-F., Champagne, O., Pergaud, J., Richard, Y., Soare, P.,
671 Pohl, B., 2018: Geomatic downscaling of temperatures in the Mont Blanc massif: A NEW
672 STATISTICAL DOWNSCALING APPROACH. *International Journal of Climatology* 38,
673 1846–1863.
- 674 Jordan, D., 2010: Le Jardin de Talèfre dans le massif du Mont-Blanc à Chamonix -
675 Réévaluation et contribution à sa connaissance botanique. *Monde Plantes* 501.

- 676 Kelly, M.A., Kubik, P.W., Von Blanckenburg, F., Schlüchter, C., 2004: Surface exposure
677 dating of the Great Aletsch Glacier Egesen moraine system, western Swiss Alps, using the
678 cosmogenic nuclide ^{10}Be . *Journal of Quaternary Science* 19, 431–441.
- 679 Kerschner, H., Hertl, A., Gross, G., Ivy-Ochs, S., Kubik, P.W., 2006: Surface exposure dating
680 of moraines in the Kromer valley (Silvretta Mountains, Austria)-evidence for glacial response
681 to the 8.2 ka event in the Eastern Alps? *The Holocene* 16, 7–15.
- 682 Kobashi, T., Severinghaus, J.P., Barnola, J.-M., 2008: 4 ± 1.5 °C abrupt warming 11,270 yr ago
683 identified from trapped air in Greenland ice. *Earth and Planetary Science Letters* 268, 397–
684 407.
- 685 Korschinek, G., Bergmaier, A., Faestermann, T., Gerstmann, U.C., Knie, K., Rugel, G.,
686 Wallner, A., Dillmann, I., Dollinger, G., von Gostomski, Ch.L., Kossert, K., Maiti, M.,
687 Poutivtsev, M., Remmert, A., 2010: A new value for the half-life of ^{10}Be by Heavy-Ion Elastic
688 Recoil Detection and liquid scintillation counting. *Nuclear Instruments and Methods in Physics*
689 *Research Section B: Beam Interactions with Materials and Atoms* 268, 187–191.
- 690 Le Roy, M., 2012: Reconstitution des fluctuations glaciaires Holocènes dans les Alpes
691 occidentales : apports de la dendrochronologie et de la datation par isotopes cosmogéniques
692 produits in situ (PhD thesis). Université Grenoble Alpes.
- 693 Le Roy, M., Deline, P., Carcaillet, J., Schimmelpfennig, I., Ermini, M., 2017: ^{10}Be exposure
694 dating of the timing of Neoglacial glacier advances in the Ecrins-Pelvoux massif, southern
695 French Alps. *Quaternary Science Reviews* 178, 118–138.
- 696 Le Roy, M., Nicolussi, K., Deline, P., Astrade, L., Edouard, J.-L., Miramont, C., Arnaud, F.,
697 2015: Calendar-dated glacier variations in the western European Alps during the Neoglacial:
698 the Mer de Glace record, Mont Blanc massif. *Quaternary Science Reviews* 108, 1–22.
- 699 Lotter, A.F., Birks, H.J.B., Eicher, U., Hofmann, W., Schwander, J., Wick, L., 2000: Younger
700 Dryas and Allerød summer temperatures at Gerzensee (Switzerland) inferred from fossil pollen

- 701 and cladoceran assemblages. *Palaeogeography, Palaeoclimatology, Palaeoecology* 159, 349–
702 361.
- 703 Maisch, M., 1981: Glazialmorphologische und gletschergeschichtliche Untersuchungen im
704 Gebiet zwischen Landwasser- und Albulatal (Kt. Graubünden, Schweiz).
- 705 Marsicek, J., Shuman, B.N., Bartlein, P.J., Shafer, S.L., Brewer, S., 2018: Reconciling
706 divergent trends and millennial variations in Holocene temperatures. *Nature* 554, 92–96.
- 707 Martin, L.C.P., Blard, P.-H., Balco, G., Lavé, J., Delunel, R., Lifton, N., Laurent, V., 2017: The
708 CREp program and the ICE-D production rate calibration database: A fully parameterizable
709 and updated online tool to compute cosmic-ray exposure ages. *Quaternary Geochronology* 38,
710 25–49.
- 711 Merchel, S., Arnold, M., Aumaître, G., Benedetti, L., Bourlès, D.L., Braucher, R., Alfimov, V.,
712 Freeman, S.P.H.T., Steier, P., Wallner, A., 2008: Towards more precise ¹⁰Be and ³⁶Cl data
713 from measurements at the 10–14 level: Influence of sample preparation. *Nuclear Instruments
714 and Methods in Physics Research Section B: Beam Interactions with Materials and Atoms* 266,
715 4921–4926.
- 716 Moran, A.P., Ivy-Ochs, S., Schuh, M., Christl, M., Kerschner, H., 2016a: Evidence of central
717 Alpine glacier advances during the Younger Dryas–early Holocene transition period. *Boreas*
718 45, 398–410.
- 719 Moran, A.P., Kerschner, H., Ochs, S.I., 2016b: Redating the moraines in the Kromer Valley
720 (Silvretta Mountains)—New evidence for an early Holocene glacier advance. *The Holocene* 26,
721 655–664.
- 722 Oerlemans, J., 2005: Extracting a Climate Signal from 169 Glacier Records. *Science* 308, 675–
723 677.
- 724 Protin, M., Schimmelpfennig, I., Mugnier, J.-L., Ravanel, L., Le Roy, M., Deline, P., Favier,
725 V., Buoncristiani, J.-F., Aumaître, G., Bourlès, D.L., Keddadouche, K., 2019 : Climatic

726 reconstruction for the Younger Dryas/Early Holocene transition and the Little Ice Age based
727 on paleo-extents of Argentière glacier (French Alps). *Quaternary Science Reviews* 221,
728 105863.

729 Prud'homme, C., Vassallo, R., Crouzet, C., Carcaillet, J., Mugnier, J.-L., Cortés-Aranda, J.,
730 2020: Paired ^{10}Be sampling of polished bedrock and erratic boulders to improve dating of
731 glacial landforms: an example from the Western Alps. *Earth Surface Processes and Landforms*
732 45, 1168–1180.

733 Putnam, A.E., Bromley, G.R.M., Rademaker, K., Schaefer, J.M., 2019: In situ ^{10}Be
734 production-rate calibration from a ^{14}C -dated late-glacial moraine belt in Rannoch Moor,
735 central Scottish Highlands. *Quaternary Geochronology* 50, 109–125.

736 Rabatel, A., Letréguilly, A., Dedieu, J.-P., Eckert, N., 2013: Changes in glacier equilibrium-
737 line altitude in the western Alps from 1984 to 2010: evaluation by remote sensing and modeling
738 of the morpho-topographic and climate controls. *The Cryosphere* 7, 1455–1471.

739 Rainsley, E., Menviel, L., Fogwill, C.J., Turney, C.S.M., Hughes, A.L.C., Rood, D.H., 2018:
740 Greenland ice mass loss during the Younger Dryas driven by Atlantic Meridional Overturning
741 Circulation feedbacks. *Scientific Reports* 8, 11307.

742 Rasmussen, S.O., Andersen, K.K., Svensson, A.M., Steffensen, J.P., Vinther, B.M., Clausen,
743 H.B., Siggaard-Andersen, M.L., Johnsen, S.J., Larsen, L.B., Dahl-Jensen, D., Bigler, M.,
744 Rothlisberger, R., Fischer, H., Goto-Azuma, K., Hansson, M.E., Ruth, U., 2006: A new
745 Greenland ice core chronology for the last glacial termination. *Journal of Geophysical Research*
746 - *Atmospheres* 111, D06102.

747 Rasmussen, S.O., Seierstad, I.K., Andersen, K.K., Bigler, M., Dahl-Jensen, D., Johnsen, S.J.,
748 2008: Synchronization of the NGRIP, GRIP, and GISP2 ice cores across MIS 2 and
749 palaeoclimatic implications. *Quaternary Science Reviews* 27, 18–28.

750 Reitner, J.M., Ivy Ochs, S., Dreschner-Schneider, R., Hajdas, I., Linner, M., 2016:

- 751 Reconsidering the current stratigraphy of the Alpine Lateglacial: Implications of the
 752 sedimentary and morphological record of the Lienz area (Tyrol/Austria). *E&G Quaternary*
 753 *Science Journal* 65, 113-144.
- 754 Renssen, H., Isarin, R.F.B., 2001: The two major warming phases of the last deglaciation at
 755 ~14.7 and ~11.5 ka cal BP in Europe: climate reconstructions and AGCM experiments. *Global*
 756 *and Planetary Change* 30, 117–153.
- 757 Renssen, H., Mairesse, A., Goosse, H., Mathiot, P., Heiri, O., Roche, D.M., Nisancioglu, K.H.,
 758 Valdes, P.J., 2015 : Multiple causes of the Younger Dryas cold period. *Nature Geoscience* 8,
 759 946–949.
- 760 Roe, G.H., Baker, M.B., Herla, F., 2017: Centennial glacier retreat as categorical evidence of
 761 regional climate change. *Nature Geoscience* 10, 95–99.
- 762 Schenk, F., Väliranta, M., Muschitiello, F., Tarasov, L., Heikkilä, M., Björck, S., Brandefelt,
 763 J., Johansson, A.V., Näslund, J.-O., Wohlfarth, B., 2018: Warm summers during the Younger
 764 Dryas cold reversal. *Nature Communications* 9, 1634.
- 765 Schimmelpfennig, I., Le Roy, M., Deline, P., Schoeneich, P., Carcaillet, J., Bodin, X., Team,
 766 A., 2019: Holocene dynamics of Arsine glacier (Ecrins massif, French Alps) inferred from ¹⁰Be
 767 dating. INQUA, Dublin. [DOI: 10.13140/RG.2.2.10849.86884](https://doi.org/10.13140/RG.2.2.10849.86884),
- 768 Schimmelpfennig, I., Schaefer, J.M., Akçar, N., Koffman, T., Ivy-Ochs, S., Schwartz, R.,
 769 Finkel, R.C., Zimmerman, S., Schlüchter, C., 2014: A chronology of Holocene and Little Ice
 770 Age glacier culminations of the Steingletscher, Central Alps, Switzerland, based on high-
 771 sensitivity beryllium-10 moraine dating. *Earth and Planetary Science Letters* 393, 220–230.
- 772 Schimmelpfennig, I., Schaefer, J.M., Goehring, B.M., Lifton, N., Putnam, A.E., Barrell, D.J.A.,
 773 2012: Calibration of the in situ cosmogenic ¹⁴C production rate in New Zealand's Southern
 774 Alps. *Journal of Quaternary Science* 27, 671–674.
- 775 Schindelwig, I., Akçar, N., Kubik, P.W., Schlüchter, C., 2012: Lateglacial and early Holocene

Mis en forme : Français (France)

776 dynamics of adjacent valley glaciers in the Western Swiss Alps. *Journal of Quaternary Science*
777 27, 114–124.

778 Schwander, J., Eicher, U., Ammann, B., 2000: Oxygen isotopes of lake marl at Gerzensee and
779 Leysin (Switzerland), covering the Younger Dryas and two minor oscillations, and their
780 correlation to the GRIP ice core. *Palaeogeography, Palaeoclimatology, Palaeoecology* 159,
781 203–214.

782 Shakun, J.D., Clark, P.U., He, F., Lifton, N.A., Liu, Z., Otto-Bliesner, B.L., 2015: Regional and
783 global forcing of glacier retreat during the last deglaciation. *Nature Communications* 6, 8059.

784 Smiraglia, C., Azzoni, R.S., D'Agata, C., Maragno, D., Fugazza, D., Diolaiuti, G.A., 2015: The
785 evolution of the Italian glaciers from the previous data base to the New Italian Inventory.
786 Preliminary considerations and results. *Geografia Fisica e Dinamica Quaternaria* 38, 79–87.

787 Solomina, O.N., Bradley, R.S., Hodgson, D.A., Ivy-Ochs, S., Jomelli, V., Mackintosh, A.N.,
788 Nesje, A., Owen, L.A., Wanner, H., Wiles, G.C., Young, N.E., 2015: Holocene glacier
789 fluctuations. *Quaternary Science Reviews* 111, 9–34.

790 Vincent, C., Fischer, A., Mayer, C., Bauder, A., Galos, S.P., Funk, M., Thibert, E., Six, D.,
791 Braun, L., Huss, M., 2017 : Common climatic signal from glaciers in the European Alps over
792 the last 50 years. *Geophysical Research Letters* 44, 1376-1383.

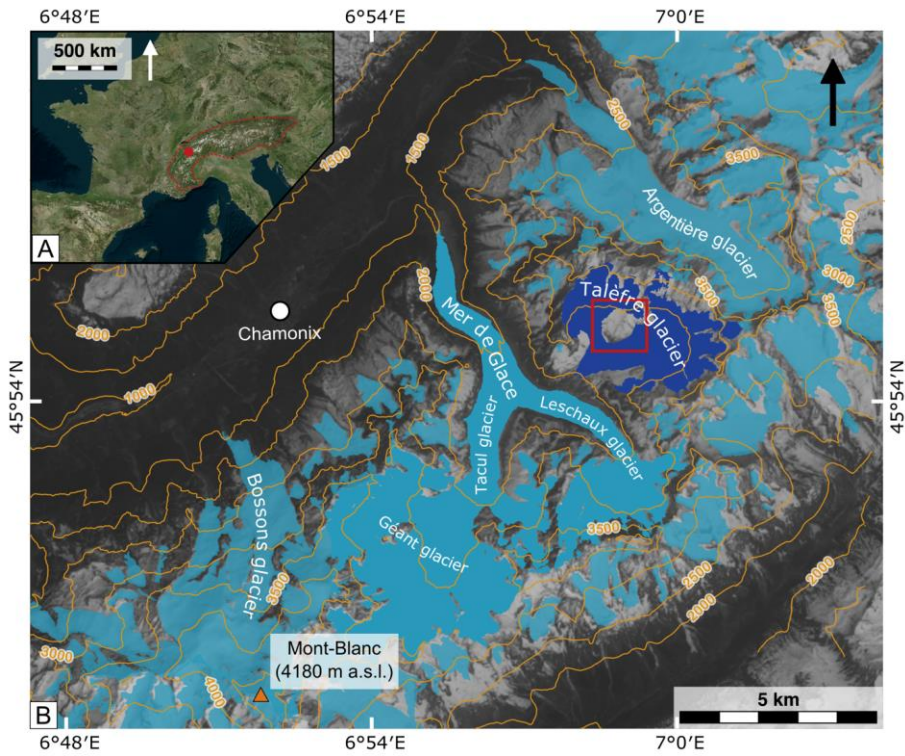
793 Vinther, B.M., Clausen, H.B., Johnsen, S.J., Rasmussen, S.O., Andersen, K.K., Buchardt, S.L.,
794 Dahl-Jensen, D., Seierstad, I.K., Siggaard-Andersen, M.-L., Steffensen, J.P., Svensson, A.,
795 Olsen, J., Heinemeier, J., 2006: A synchronized dating of three Greenland ice cores throughout
796 the Holocene. *Journal of Geophysical Research - Atmospheres* 111, D13102.

797 Ward, G.K., Wilson, S.R., 1978: Procedures for comparing and combining radiocarbon age
798 determinations: a critique. *Archaeometry* 20, 19–31.

799 Wittmeier, H.E., Schaefer, J.M., Bakke, J., Rupper, S., Paasche, Ø., Schwartz, R., Finkel, R.C.,
800 2020: Late Glacial mountain glacier culmination in Arctic Norway prior to the Younger Dryas.

- 801 *Quaternary Science Reviews* 245, 106461.
- 802 Wurth, G., Niggemann, S., Richter, D.K., Mangini, A., 2004: The Younger Dryas and Holocene
803 climate record of a stalagmite from Hölloch Cave(Bavarian Alps, Germany. *Journal of*
804 *Quaternary Science* 19, 291–298.
- 805 Young, N.E., Briner, J.P., Miller, G.H., Lesnek, A.J., Crump, S.E., Thomas, E.K., Pendleton,
806 S.L., Cuzzone, J., Lamp, J., Zimmerman, S., Caffee, M., Schaefer, J.M., 2020: Deglaciation of
807 the Greenland and Laurentide ice sheets interrupted by glacier advance during abrupt coolings.
808 *Quaternary Science Reviews* 229, 106091.
- 809 Young, N.E., Briner, J.P., Schaefer, J., Zimmerman, S., Finkel, R.C., 2019: Early Younger
810 Dryas glacier culmination in southern Alaska: Implications for North Atlantic climate change
811 during the last deglaciation. *Geology* 47, 550–554.
- 812 Young, N.E., Schaefer, J.M., Briner, J.P., Goehring, B.M., 2013. A ^{10}Be production-rate
813 calibration for the Arctic. *Journal of Quaternary Science* 28, 515–526.
- 814

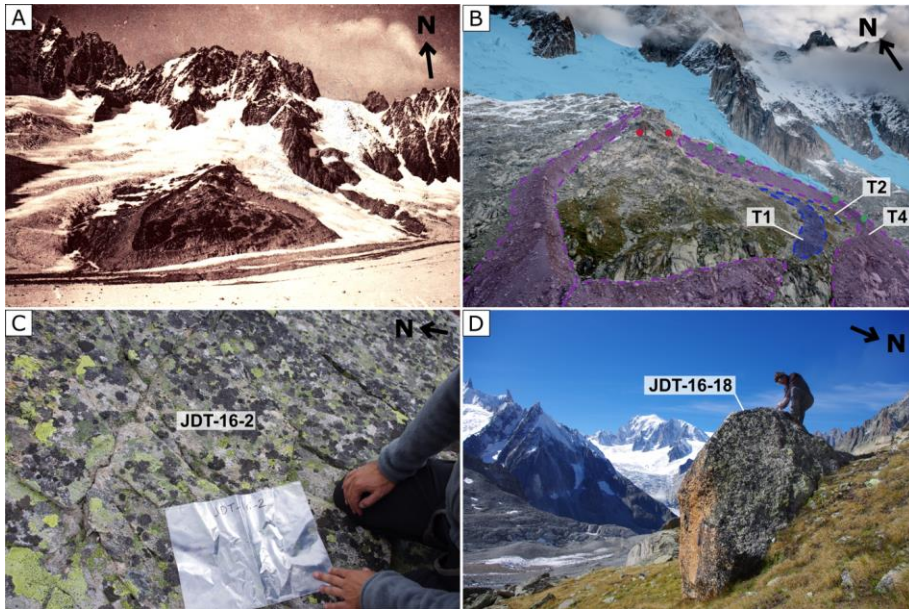
815 Figures



816

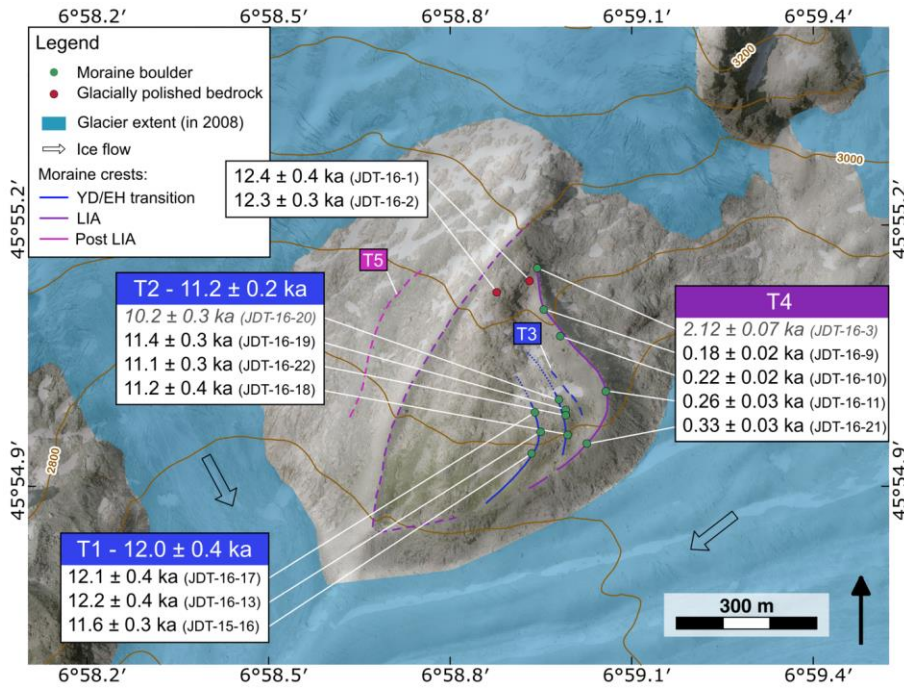
817 Fig. 1: Location of Talèfre glacier and study area: the “Jardin de Talèfre”. (A) Location of the
 818 Mont Blanc massif (red dot) in the Alps (red dotted line). (B) The Mont Blanc massif and
 819 present-day glacier extents on a Landsat 8 image (April 2015); French glaciers: Gardent et al.
 820 (2014); Swiss glaciers: Fischer et al. (2014); Italian glaciers: Smiraglia et al. (2015). Talèfre
 821 glacier is highlighted in dark blue, the “Jardin de Talèfre” is located in the red square.

822

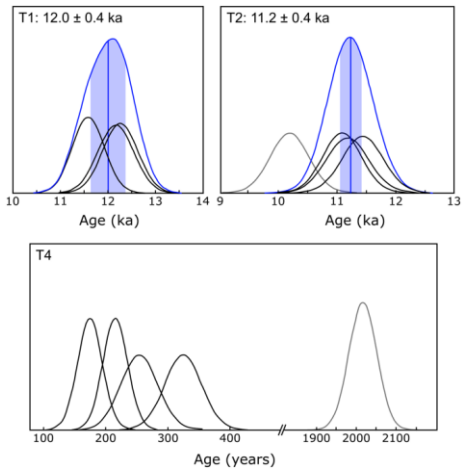


823
 824 Fig. 2: (A) Photography of the « Jardin de Talèfre » in 1890 C.E. (source: "Les Amis du Vieux
 825 Chamonix"); (B) oblique aerial photography imagery of the "Jardin de Talèfre" in September
 826 2016; Talèfre glacier is highlighted in light blue, sampled moraines T1 and T2 (dark blue) and
 827 Holocene moraines, including T4 (purple); bedrock sample locations are shown as red dots and
 828 some of the sampled boulders as green dots (photograph by J.F. Buoncristiani); (C) example
 829 of sampled bedrock surface; (D) example of sampled boulder on T2 moraine.

830



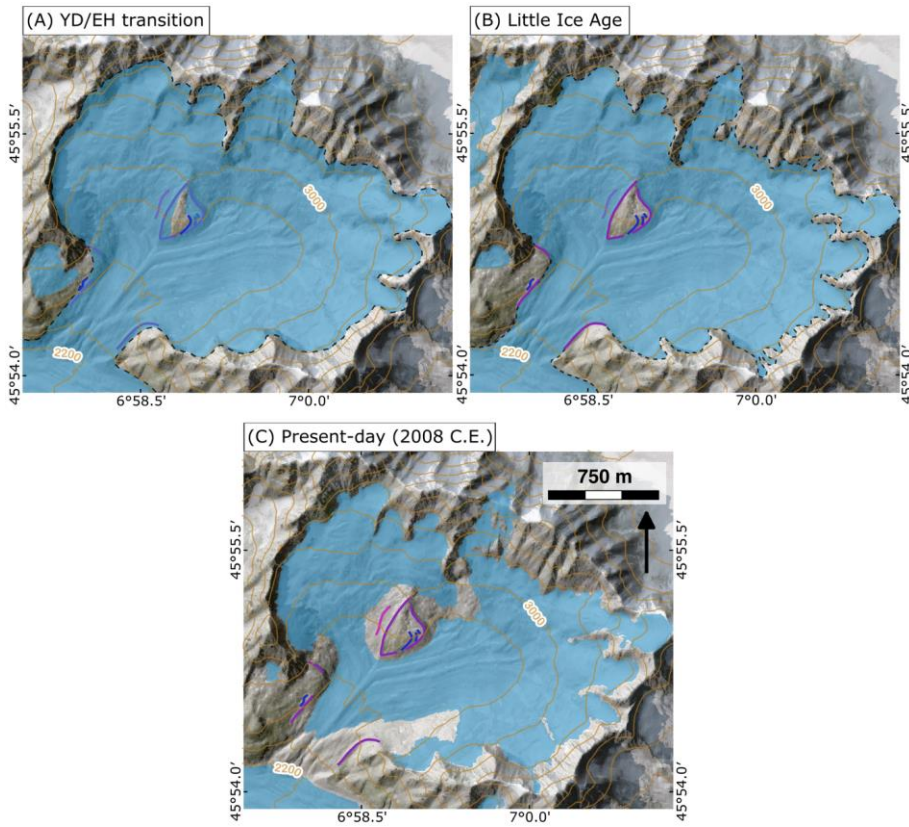
831
 832 Fig. 3: Moraines and sample locations in the “Jardin de Talèfre”, mapped on the 5 m IGN DEM
 833 RGE ALTI and aerial images. Present-day glacier extent (in blue) is from Gardent et al. (2014).
 834 Dashed lines represent undated moraines, the age of which is assumed according to their
 835 relative position and morphology appearance. Individual surface exposure ages are listed in the
 836 white boxes with their analytical uncertainties and mean ages of the landforms in the colored
 837 bands (arithmetic means and standard deviations). ~~Outlier~~Outliers are in italic grey font.
 838



839

840 Fig. 4: Probability plots of the individual moraine sample ages (black curves, analytical
 841 uncertainty only) from Talèfre glacier. Colored curves, vertical lines and bands represent the
 842 summed probability plots, arithmetic means and standard deviations, respectively,
 843 corresponding to the age labeled in each box, only calculated for T1 and T2.

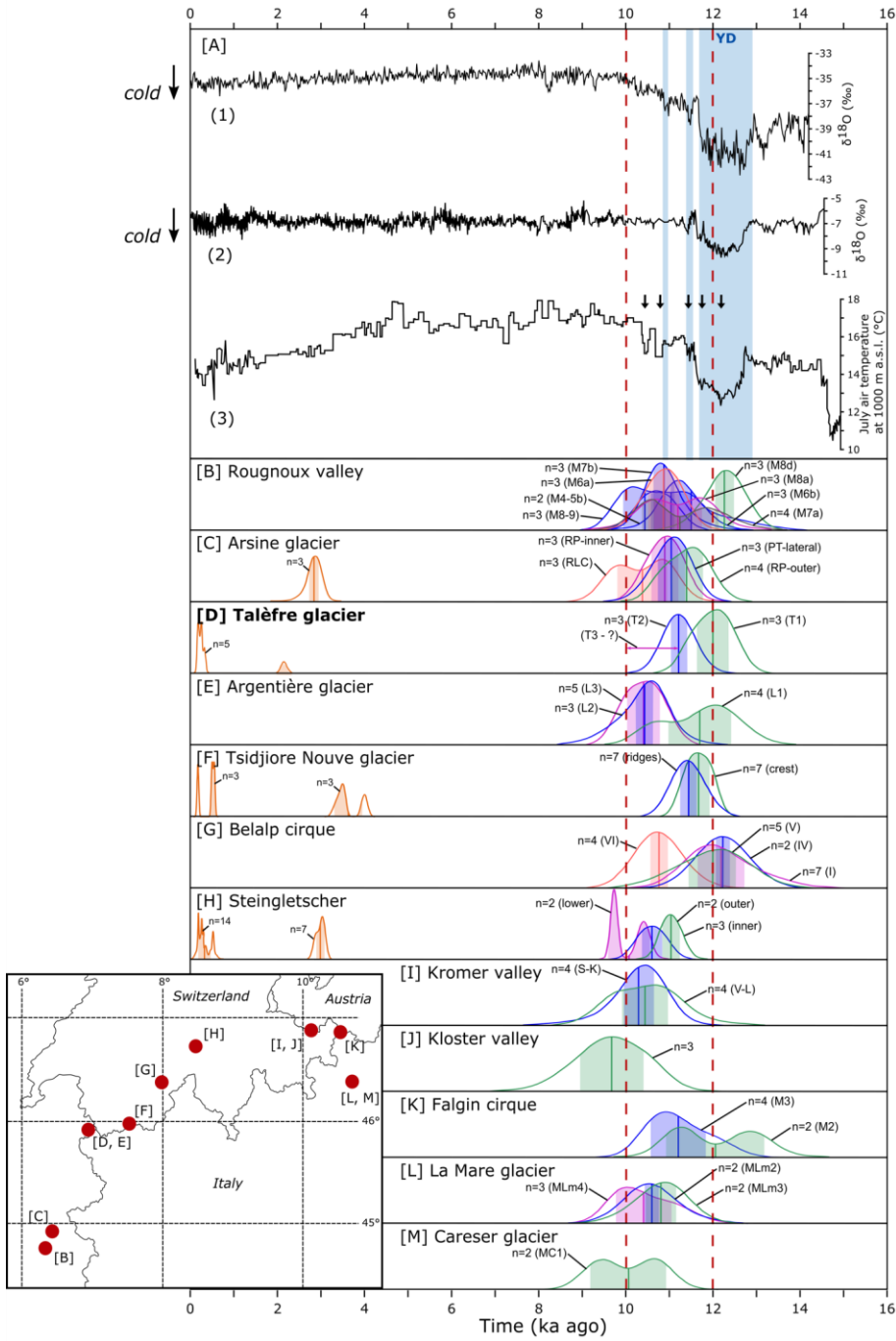
844



845

846 Fig. 5: Estimation-Reconstruction of past extents of Talèfre glacier, based on mapping of the preserved
 847 moraines and interpretation of ^{10}Be dating, for the (A) during the Younger Dryas/Early
 848 Holocene transition (12 ka, stage T1 moraine), (B) LIA maximum and (C) 2008 C.E. (Gardent
 849 et al., 2014). Dashed glacier limits correspond to hypothetic extents.

850



852 Fig. 6: Chronology of culminations of Talèfre glacier based on the ^{10}Be mean ages of the glacial
 853 landforms in this study [panel D] compared to independent paleoclimate records [panel A] and
 854 to other glacier chronology studies in the Alps also using ^{10}Be moraine dating [panels B to M].
 855 Each moraine is represented by a summed probability curve along with the number of dated
 856 boulders ($n=x$), vertical lines and colored band represent the arithmetic means and standard
 857 deviations (1σ), colors represent the stratigraphic order of the moraines (from outer to inner:
 858 green, blue, purple, pink). Panel [A]: (1) Oxygen isotope record in Greenland ice core NGRIP
 859 (Rasmussen et al., 2006; Vinther et al., 2006), blue bands represent the Younger Dryas and cold
 860 peaks during the Early Holocene as identified in the Greenland ice core record, (2) Oxygen
 861 isotope record from speleotem fluid inclusion from Milandre cave, Switzerland (Affolter et al.,
 862 2019) (3) Stacked chironomid-inferred July air temperature from the Alps (Heiri et al., 2015),
 863 black arrows point to peaks mentioned in the main text. Alpine glacier sites in panels [B], [C]
 864 and [E] to [M] are presented from east to west with their locations shown by red dots on the
 865 map. [B] Rougnoux valley (Hofmann, 2018), [C] Arsine glacier (Schimmelpfennig et al., 2019;
 866 Le Roy et al., in prep), [E] Argentière glacier (Protin et al., 2019), [F] Tsidjiore Nouve glacier
 867 (Schimmelpfennig et al., 2012), [G] Belalp cirque (Schindelwig et al., 2012), [H] Steingletscher
 868 (Schimmelpfennig et al., 2014), [I] Kromer valley (Kerschner et al., 2006; Moran et al., 2016b),
 869 [J] Kloster valley (Moran et al., 2016b), [K] Falgin glacier (Moran et al., 2016a), [L] La Mare
 870 glacier (Baroni et al., 2017) and [M] Careser glacier (Baroni et al., 2017). Vertical dashed lines
 871 delimit the YD/EH transition period between 12 and 10 ka ago.

872

873 Tables

874 Table 1: Characteristics and ^{10}Be measurement details of samples [A] and blanks [B] carried
 875 out for this study. Outliers are highlighted by (O). Mean landform ages of T1 and T2 are

876 indicated with standard deviations and total uncertainties (including the ^{10}Be production rate
877 uncertainty) in parentheses.

Commenté [MOU15]: Marie, add the Artic PR ages

Sample name	Latitude (dd)	Longitude (dd)	Altitude (m a.s.l.)	Thickness (mm)	Shielding factor	Quartz weight (g)	Carrier (mg ⁹ Be)	Associated blank	¹⁰ Be/ ⁹ Be x10 ⁻¹⁴	[¹⁰ Be] (x10 ⁴ at.g ⁻¹)	¹⁰ Be age (ka)	1σ analytical uncertainty y (ka)	1σ total uncertainty (ka)
MORaine SAMPLES													
T1												11.97 ± 0.36 (0.4)	
JDT-16-17	45.91642	6.98233	2825	45	0.9063	24.67	0.3053	15Jan18	44.9 ± 1.4	36.8 ± 1.2	12.14	0.37	0.47
JDT-16-13	45.91604	6.98249	2817	27	0.9635	15.35	0.3072	15Jan18	30.13 ± 0.93	39.8 ± 1.2	12.21	0.36	0.46
JDT-16-16	45.91564	6.98224	2798	22	0.9635	28.65	0.3078	15Jan18	52.3 ± 1.6	37.3 ± 1.2	11.56	0.34	0.42
T2												11.21 ± 0.17 (0.28)	
JDT-16-20 (O)	45.91667	6.98301	2835	42	0.9638	26.58	0.3071	15Jan18	42.7 ± 1.4	32.7 ± 1.1	10.15	0.32	0.4
JDT-16-19	45.91647	6.98318	2827	25	0.9638	21.49	0.3070	15Jan18	39.5 ± 1.3	37.4 ± 1.2	11.40	0.34	0.43
JDT-16-22	45.91636	6.98320	2824	24	0.9638	32.44	0.3069	15Jan18	57.6 ± 1.8	36.2 ± 1.1	11.07	0.33	0.41
JDT-16-18	45.91599	6.98324	2805	35	0.9527	20.18	0.3083	15Jan18	34.9 ± 1.2	35.3 ± 1.2	11.15	0.35	0.44
T4													
JDT-16-3 (O)	45.91918	6.98241	2951	20	0.9677	37.83	0.3048	08Dec17	13.43 ± 0.42	7.05 ± 0.23	2.12	0.07	0.09
JDT-16-9	45.91840	6.98260	2923	38	0.9625	31.65	0.3033	08Dec17	1.33 ± 0.11	0.64 ± 0.08	0.18	0.02	0.02
JDT-16-10	45.91788	6.98305	2903	28	0.9625	31.26	0.3017	08Dec17	1.56 ± 0.11	0.78 ± 0.08	0.22	0.02	0.02
JDT-16-11	45.91683	6.98430	2842	26	0.9434	36.61	0.3063	08Dec17	1.88 ± 1.2	0.86 ± 0.07	0.26	0.03	0.03

JDT-16-21	45.91583	6.98377	2796	22	0.9623	33.60	0.3010	08Dec17	2.16 ± 0.12	1.09 ± 0.08	0.33	0.03	0.03
-----------	----------	---------	------	----	--------	-------	--------	---------	-----------------	-----------------	------	------	------

BEDROCK SAMPLES

JDT-16-1	45.91873	6.98128	2950	32	0.9667	20.09	0.3015	08Dec17	44.2 ± 1.4	44.0 ± 1.4	12.43	0.38	0.48
----------	----------	---------	------	----	--------	-------	--------	---------	----------------	----------------	-------	------	------

JDT-16-2	45.91894	6.98219	2943	26	0.9677	17.83	0.3048	08Dec17	38.6 ± 1.1	43.7 ± 1.2	12.31	0.33	0.44
----------	----------	---------	------	----	--------	-------	--------	---------	----------------	----------------	-------	------	------

Blanks

Blank name	Carrier (mg ^9Be)	$^{10}\text{Be}/^9\text{Be} \times 10^{-14}$	Number of ^{10}Be atoms ($\times 10^4$ at)
8Dec17	0.3040	0.338 ± 0.049	6.9 ± 1.0
15Jan18	0.3075	0.348 ± 0.050	7.2 ± 1.0